Human Fetal TNF-α-Cytokine-Producing CD4 + Effector Memory T Cells Promote Intestinal Development and Mediate Inflammation Early in Life

Schreurs, Renée R. C. E.; Baumdick, Martin E.; Sagebiel, Adrian F.; Kaufmann, Max; Mokry, Michal; Klarenbeek, Paul L.; Schaltenberg, Nicola; Steinert, Fenja L.; van Rijn, Jorik M.; Drewniak, Agata; The, Sarah-May M. L.; Bakx, Roel; Derikx, Joep P. M.; de Vries, Niek; Corpeleijn, Willemijn E.; Pals, Steven T.; Gagliani, Nicola; Friese, Manuel A.; Middendorp, Sabine; Nieuwenhuis, Edward E. S.; Reinshagen, Konrad; Geijtenbeek, Teunis B. H.; van Goudoever, Johannes B.; Bunders, Madeleine J.

Published in:
Immunity

DOI:
10.1016/j.immuni.2018.12.010

Published: 19/02/2019

Document Version
Peer reviewed version

Citation for pulished version (APA):
Schreurs, R. R. C. E., Baumdick, M. E., Sagebiel, A. F., Kaufmann, M., Mokry, M., Klarenbeek, P. L., Schaltenberg, N., Steinert, F. L., van Rijn, J. M., Drewniak, A., The, S.-M. M. L., Bakx, R., Derikx, J. P. M., de Vries, N., Corpeleijn, W. E., Pals, S. T., Gagliani, N., Friese, M. A., Middendorp, S., ... Bunders, M. J. (2019). Human Fetal TNF-α-Cytokine-Producing CD4 + Effector Memory T Cells Promote Intestinal Development and Mediate Inflammation Early in Life. *Immunity*, *50*(2), 462-476.e8. https://doi.org/10.1016/j.immuni.2018.12.010

Development of intestinal immunity

Spilling the guts on T cell maturation and inflammation in the early-life intestine

Schreurs, R.R.C.E.

Publication date
2021

CHAPTER 4

HUMAN FETAL TNF-α-CYTOKINE-PRODUCING CD4^{+} EFFECTOR MEMORY T CELLS PROMOTE INTESTINAL DEVELOPMENT AND MEDIATE INFLAMMATION EARLY IN LIFE

Renée R.C.E. Schreurs[1,2], Martin E. Baumdick[3,17], Adrian F. Sagebiel[3,17], Max Kaufmann[4], Michal Mokry[5,6], Paul L. Klarenbeek[7,8], Nicola Schaltenberg[9,10], Fenja L. Steinert[3], Jorik M. van Rijn[5,6], Agata Drewniak[1,11], Sarah-May M.L. The[1,12], Roel Bakx[12], Joep P.M. Derikx[12], Niek de Vries[7,8], Willemijn E. Corpeleijn[2], Steven T. Pals[13], Nicola Gagliani[9,14], Manuel A. Friese[4], Sabine Middendorp[5,6], Edward E.S. Nieuwenhuis[5,6], Konrad Reinshagen[15], Teunis B.H. Geijtenbeek[1], Johannes B. van Goudoever[2,16], and Madeleine J. Bunders[1,2,3]

[1] Department of Experimental Immunology, Amsterdam Infection & Immunity Institute (AI&II), Amsterdam University Medical Center (AUMC), University of Amsterdam (UvA), Amsterdam, the Netherlands; [2] Department of Pediatrics, Emma Children's Hospital, AUMC, UvA, Amsterdam, the Netherlands; [3] Heinrich Pette Institute, Leibniz Institute for Experimental Virology, Hamburg, Germany; [4] Institut für Neuroimmunologie und Multiple Sklerose, Zentrum für Molekulare Neurobiologie Hamburg, Universitätsklinikum Hamburg-Eppendorf (UKE), Hamburg, Germany; [5] Division of Pediatrics, Department of Pediatric Gastroenterology, Wilhelmina Children's Hospital, Utrecht University Medical Center (UMC), Utrecht University (UU), Utrecht, the Netherlands; [6] Regenerative Medicine Center Utrecht, UMC, UU, Utrecht, the Netherlands; [7] Department of Clinical Immunology and Rheumatology and Department of Experimental Immunology, AI&II, AUMC, UvA, Amsterdam, the Netherlands; [8] Amsterdam Rheumatology & Immunology Center, AUMC, UvA, Amsterdam, the Netherlands; [9] Department of General, Visceral, and Thoracic Surgery and I. Department of Medicine, UKE, Hamburg, Germany; [10] Department of Biochemistry and Molecular Cell Biology, UKE, Hamburg, Germany; [11] Kiadis Pharma B.V., Amsterdam, the Netherlands; [12] Department of Pediatric Surgery, Pediatric Surgery Center of Amsterdam, AUMC, Amsterdam, the Netherlands; [13] Department of Pathology, AUMC, UvA, Amsterdam, the Netherlands; [14] Immunology and Allergy Unit, Department of Medicine Solna, Karolinska Institute, Stockholm, Sweden; [15] Department of Pediatric Surgery, UKE, Hamburg, Germany; [16] Department of Pediatrics, Emma Children's Hospital, AUMC, Vrije Universiteit, Amsterdam, the Netherlands; [17] These authors contributed equally

Immunity (2019) 50 (2), 462-476

SUMMARY

Although the fetal immune system is considered tolerogenic, preterm infants can suffer from severe intestinal inflammation, including necrotizing enterocolitis (NEC). Here, we demonstrate that human fetal intestines predominantly contain tumor necrosis factor-α (TNF-α)$^{+}$CD4^{+}CD69^{+} T effector memory (Tem) cells. Single-cell RNA sequencing of fetal intestinal CD4^{+} T cells showed a T helper 1 phenotype and expression of genes mediating epithelial growth and cell cycling. Organoid co-cultures revealed a dose dependent, TNF-α-mediated effect of fetal intestinal CD4^{+} T cells on intestinal stem cell (ISC) development, in which low T cell numbers supported epithelial development, whereas high numbers abrogated ISC proliferation. CD4^{+} Tem cell frequencies were higher in inflamed intestines from preterm infants with NEC than in healthy infant intestines and showed enhanced TNF signaling. These findings reveal a distinct population of TNF-α-producing CD4^{+} T cells that promote mucosal development in fetal intestines but can also mediate inflammation upon preterm birth.

GRAPHICAL SUMMARY

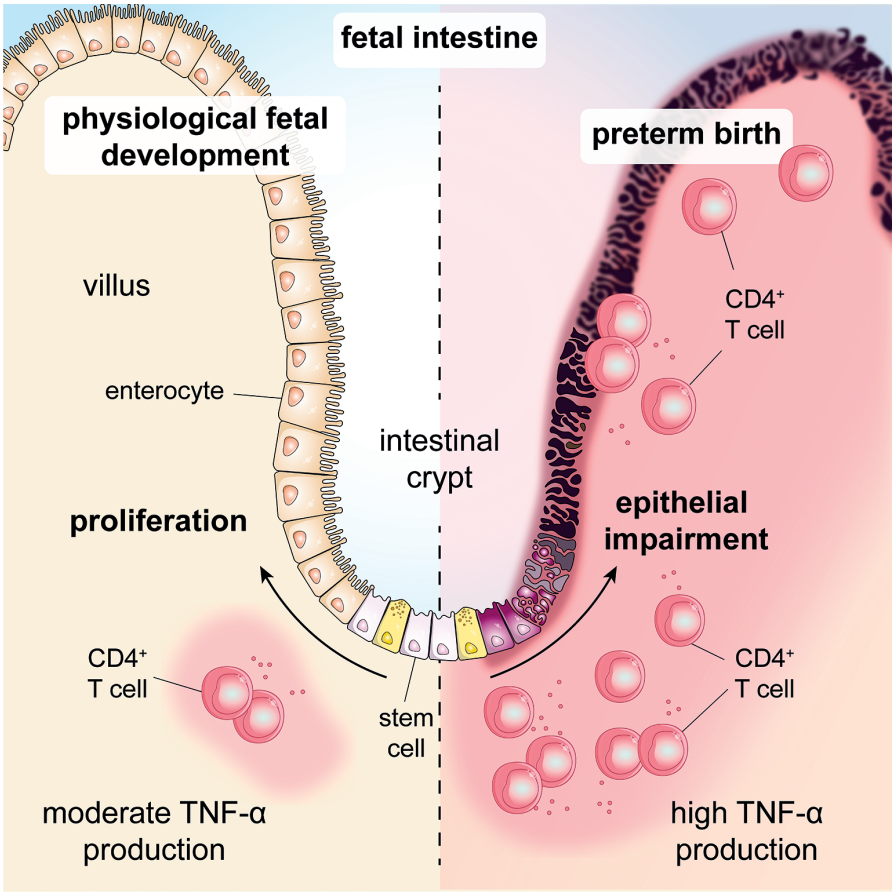

INTRODUCTION

Immunity in early life is faced with extraordinary challenges, including upholding of the fetal-maternal equilibrium and avoiding fetus-against-mother responses, unmatched tissue growth, and adaptation to imminent microbial invasion at birth. Studies of cord and infant blood have shown that the infant immune system is characterized by T regulatory (Treg) and T helper 2 (Th2) cells, whereas Th1 cell responses are limited early in life (Michäelsson et al., 2006; Prendergast et al., 2012; Zhang et al., 2014). Further studies of fetal tissues have shown that this bias toward Treg and Th2 cells already exists from the second trimester of gestation in fetal spleens and lymph nodes (Mold et al., 2008). Several mechanisms have been proposed for the relative tolerance of the fetal immune system (He et al., 2018; McGovern et al., 2017; Mold et al., 2008). In a recent study, the differential expression of arginase-2 between fetal splenic dendritic cells (DCs) and adult splenic DCs revealed that fetal DCs favor induction of Treg and Th2 cells over Th1 cells (McGovern et al., 2017). Although the infant immune system clearly differs from the adult immune system, there are suggestions that it is not anti-inflammatory only, because a population of proinflammatory CXCL8-chemokine-producing T cells has been described in infant blood (Gibbons et al., 2014).

Studies in adults have shown distinct compartmentalization of tissue-resident memory T (Trm) cells (Masopust et al., 2010; Mueller and Mackay, 2016). We have previously demonstrated that $CD4^+CD45R0^+$ T cells are abundantly present in human intestines, but not in blood, at birth and display tissue-specific expression of chemokine receptors (Bunders et al., 2012). Furthermore, $CD4^+$ T cell clones in the infant intestine are highly compartmentalized and have limited overlap with clones in the spleen or blood (Bunders et al., 2012), suggesting that the intestine might harbor a distinctive tissue-resident population of memory $CD4^+$ T cells prior to birth. This observation is supported by subsequent studies describing infant intestines with large numbers of memory $CD4^+$ T cells that express CD69, which allows these cells to remain tissue resident (Thome et al., 2016). Because the classical task of T cells in host defense is negligible prior to birth, the physiological role of $CD4^+CD45R0^+$ T cells in the intestine so early during human development remains unclear. There is an increasing appreciation for the effects of cytokines produced by tissue-resident lymphocytes to support tissue regeneration (Karin and Clevers, 2016). For example, interleukine-22 (IL-22), a cytokine produced by innate intestinal lymphocytes, can contribute to the growth of the intestinal epithelium by inducing proliferation of intestinal stem cells (ISCs) (Lindemans et al., 2015). However, inadequate control of immune responses can result in severe intestinal inflammation (Maloy and Powrie, 2011; Powrie et al., 1994). During birth, the fetus leaves the protected maternal environment and is exposed to large numbers of microbes. Strict control of proinflammatory immune responses prevents inflammation of the intestinal mucosa in most cases (Rautava et al., 2012); however, preterm birth predisposes infants to necrotizing enterocolitis (NEC), a severe intestinal inflammatory disease that has a 20% mortality rate (Neu and Walker, 2011) and does not occur in term-born infants.

In this study, we investigated the ontogeny of intestinal CD4$^+$ T cells in human fetal intestines and their effects on intestinal development. CD4$^+$ T effector memory (Tem) cells that produced tumor necrosis factor-α (TNF-α) were present very early in fetal intestines from the end of the first trimester, whereas Treg cells were scarce. Single-cell RNA sequencing (scRNA-seq) of fetal intestinal CD4$^+$ T cells revealed a Th1 cell phenotype and enhanced expression of genes in pathways regulating cell cycle and tissue development. By employing organoid co-cultures of fetal CD4$^+$ Tem cells and intestinal stem cells (ISCs), we observed that low numbers of fetal intestinal CD4$^+$ T cells supported ISC growth, whereas a high concentration of CD4$^+$ Tem cells impaired ISC development, and that these effects were mediated by TNF-α. The detrimental effect of a high concentration of TNF-α on intestinal development was in line with observations in preterm NEC-affected infants, who had increased numbers of TNF-α$^+$CD4$^+$ Tem cells and upregulated expression of TNF-induced genes in the affected intestinal tissues. Altogether, these findings demonstrate a role for intestinal TNF-α$^+$CD4$^+$ T cells in tissue generation prior to birth, whereas premature birth and exposure to the external environment can activate TNF-α-producing CD4$^+$ T cells and induce intestinal inflammation in preterm infants.

RESULTS

CD4$^+$ T cells populate the fetal intestinal mucosa early in human development

The human thymus contains CD4$^+$ T cells starting at the end of the first trimester (Haynes and Heinly, 1995); we therefore explored whether CD4$^+$ T cells were present in fetal intestines ranging from 13 to 20 weeks of gestation. At 13 weeks of gestation, the earliest time point in this study, CD3$^+$ T cells were already detected in the intestinal epithelium and lamina propria. Single-positive CD4$^+$CD8$^-$ T cells made up 36% (interquartile range [IQR] 21%–47%) of epithelium-derived T cells and 57% (IQR 51%–62%) of lamina-propria-derived T cells (**Figures 1A and 1B**). Intestinal CD4$^+$ T cells were almost all (over 95%) ab T cells (**Figure S1A**). These large numbers of CD4$^+$ T cells prior to birth were unique to the human fetal intestine because intestines of fetal mice at embryonic day 19.5 (E19.5) did not contain T cells (**Figure S1B**). Analyses of human pediatric intestinal samples obtained at surgical reconstruction of congenital abnormalities (median age 4 months) showed that epithelial CD4$^+$ T cells were still abundant at that age (**Figures 1A and 1B**). Absolute numbers of CD4$^+$ T cells per cm2 of tissue were further increased in infant intestinal tissues compared with fetal tissues (**Figures 1C and S1C**). These data demonstrate that, unlike in mice, CD4$^+$ T cells were already present early in the human fetal intestinal mucosa and that their numbers further increased with age.

Fetal intestinal CD4$^+$ T cells are predominantly effector memory T cells

In peripheral blood, T cell differentiation follows a linear pathway, starting from mostly naive CD4$^+$ T cells at birth, and requires several years (Durek et al., 2016). However, in contrast to those in fetal lymph node or cord blood, the majority of fetal intestinal CD4$^+$ T cells were CD45RA$^-$CCR7$^-$CD4$^+$ T cells, representing 73% (IQR 57%–79%) in the epithelium and 76% (IQR 72%–82%) in lamina propria tissues (**Figures 1D–1F**). Fetal intestinal CD45RA$^-$CCR7$^-$CD4$^+$ T

cells had significantly lower CD27 and CD28 expression than infant cells, indicating a phenotype further differentiated from infant intestinal CD4+ T cells (**Figure S1D**). However, a proportion of CD45RA-CCR7-CD4+ T cells expressed CD28 and, to a lesser extent, CD27, suggesting an effector memory phenotype. Furthermore, the frequencies of naive CD45RA+CCR7+CD4+ T (Tn) cells in fetal intestines were significantly lower than those in infant intestines (**Figures 1D–1F**).

The frequencies of early differentiated memory cells (including stem memory CD45RA+CCR7+CD95+CD28+CD4+ T [Tsmc] cells and central memory CD45RA-CCR7+CD4+ T [Tcm] cells), however, did not differ between fetal and infant intestines (**Figures 1D–1F**). t-distributed stochastic neighbor embedding (t-SNE) analyses of intestinal CD4+ T cells confirmed a large homogeneous cluster of CD4+ Tem cells in fetal tissue (**Figure 1E**). Because fetal intestinal CD4+ T cells showed a differentiated memory phenotype, we assessed whether fetal intestinal CD4+ T cells had undergone clonal expansion by using T cell receptor (TCR) RNA sequencing. TCR repertoires from sorted fetal intestinal CD4+ Tem cells contained expanded clones among an overall polyclonal repertoire (**Figure 1G**), demonstrating that fetal intestinal CD4+ T cells had undergone clonal expansion during fetal development and were not derived from public clones. The clonal distribution of intestinal CD4+ T cells in the infant sample was in line with our previously published data (Bunders et al., 2012). Altogether, these data demonstrate that polyclonal CD4+ T cells with a predominantly effector memory phenotype are present in fetal intestines early in human development.

Fetal intestinal CD4+ Tem cells express CD69 and CD103 but limited PD1

T cells can be anchored in tissues by specific molecules such as CD103 and CD69 (Mackay et al., 2012; Schoenberger, 2012). CD103 expression was significantly higher in fetal than in infant intestinal CD4+ Tem cells (**Figures 2A and 2B**). Similarly, CD69 was expressed by significantly more fetal lamina-propria-derived CD4+ Tem cells than infant CD4+ Tem cells ($p < 0.01$) (**Figures 2A and 2B**). t-SNE analyses showed that fetal CD69+ CD103+CD4+ Tem cells formed a separate cluster (**Figure 2C**), further indicating compartmentalization of early human T cell responses. Auto-inflammation by T cells in high antigenic environments, such as the intestinal mucosa, is prevented through several mechanisms, including inhibition of T cell effector function by programmed cell death 1 (PD1) (Sharpe et al., 2007). Frequencies of epithelium- and lamina-propria-derived PD1+CD4+ T cells were higher in infant than in fetal intestines (**Figures 2D and 2E**). PD1 expression was particularly high in infant compared with fetal intestinal CD4+CD69+ T cells ($p < 0.05$) (**Figures 2F and 2G**), indicating potential for PD1-mediated immune regulation in infant tissues. The overall low expression of PD1 in tissue-resident CD4+ Tem cells in fetal intestines suggests that there was little attenuation of intestinal fetal CD4+ T cells through PD1.

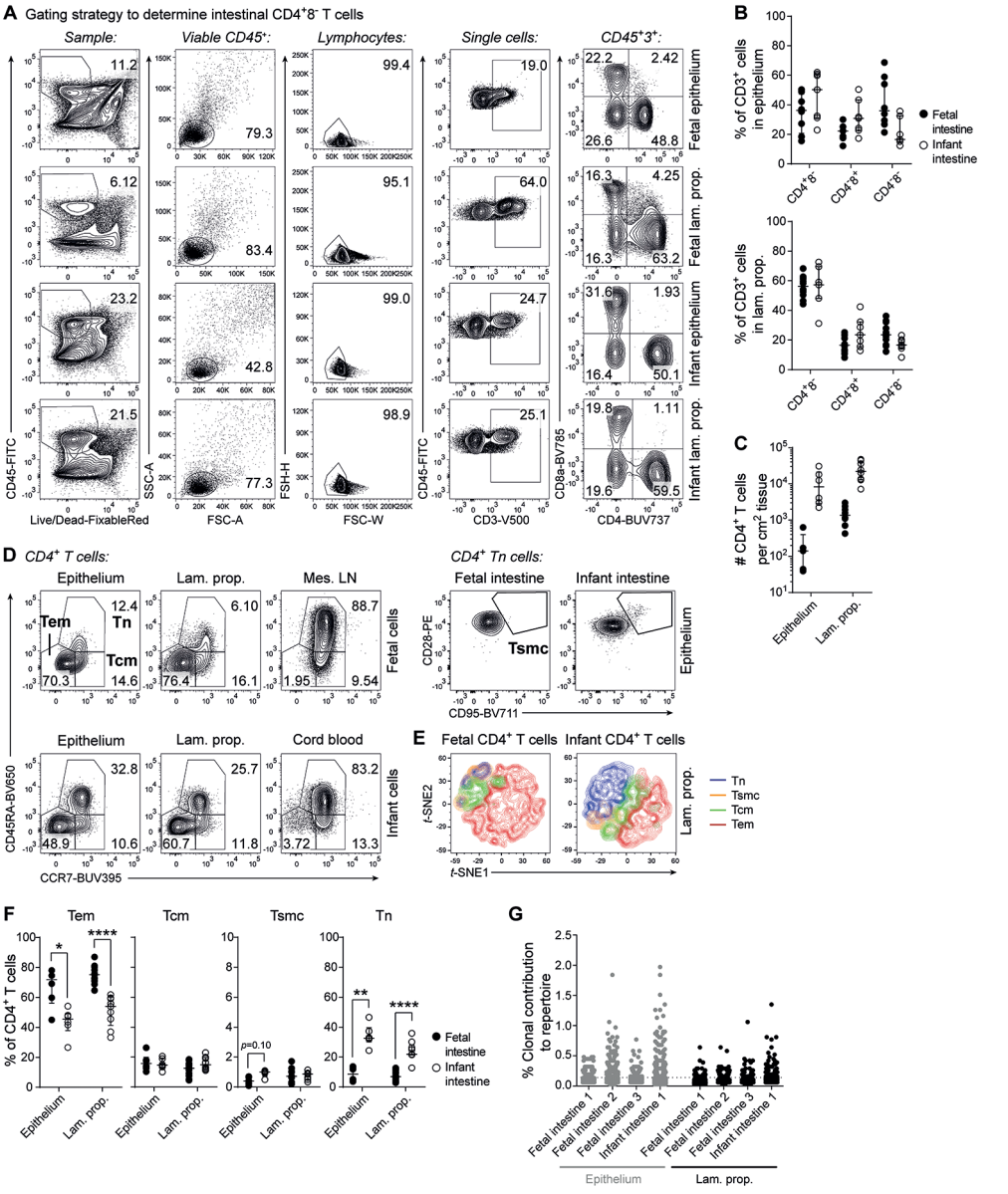

Figure 1. CD4⁺ T effector memory cells are abundant in fetal intestines. (A) Gating strategy for intestinal CD4⁺CD8⁻ T cells. (B) Median percentage (±IQR) of CD4⁺CD8⁻, CD4⁻CD8⁺, and CD4⁻CD8⁻ T cells in fetal and infant epithelium and lamina propria intestinal tissues. Shown are fetal epithelium (n = 8) and lamina propria (n = 12) samples and infant epithelium (n = 7) and lamina propria (n = 7) samples. Because of the limited numbers of cells isolated from tissues, not all experiments could be performed in all donors simultaneously. (C) Median count (±IQR) of fetal and infant epithelium- and lamina-propria-derived CD4⁺ T cells per cm² of tissue. Shown are fetal epithelium (n = 5) and lamina propria (n =8) samples and infant epithelium (n = 6) and lamina propria (n = 8) samples. (D) Flow-cytometric plots of CD45RA and CCR7 expression on CD4⁺ T cells in fetal epithelium, lamina propria, and mesenteric lymph node tissues (top) and in infant epithelium, lamina propria, and cord blood samples (bottom). CD28 and CD95 ▸

expression on epithelial CD45RA$^+$CCR7$^+$CD4$^+$ Tn cells is depicted on the right. (E) t-SNE plot of fetal and infant lamina-propria-derived CD4$^+$ T cell subsets. (F) Median percentage (±IQR) of intestinal CD4$^+$ T cell subsets CD45RA$^-$CCR7$^-$ Tem, CD45RA$^-$CCR7$^+$ Tcm, CD28$^+$CD95$^+$ Tsmc, and CD45RA$^+$CCR7$^+$ Tn (from left to right). Shown are fetal epithelium (n = 6) and lamina propria (n = 13) samples and infant epithelium (n = 6) and lamina propria (n = 9) samples. (G) TCR clones of fetal and infant epithelium- and lamina-propria-derived CD4$^+$ Tem cells. Shown are fetal epithelium (n = 3) and lamina propria (n = 3) samples and infant epithelium (n = 1) and lamina propria (n = 1) samples. The dotted line represents the cutoff of expanded T cell clones (Bunders et al., 2012; Klarenbeek et al., 2010). Statistical significance was measured by Mann-Whitney U comparisons. *p < 0.05, **p < 0.01, ***p < 0.001, ****p < 0.0001. Abbreviations are as follows: lam. prop., lamina propria; mes. LN, mesenteric lymph node; Tem, effector memory T cells; Tcm, central memory T cells; Tsmc, stem memory T cells; and Tn, naïve T cells (**Figure S1**).

CD4$^+$ T cells in fetal intestines are characterized by TNF-α production

Human adaptive CD4$^+$ T cell responses in primary lymphoid tissues from fetuses have been characterized as Treg and Th2 cell biased (McGovern et al., 2017; Michäelsson et al., 2006; Mold et al., 2008). However, fetal intestinal CD4$^+$ T cells produced more TNF-α (17.5%, IQR 16%–19%; $p < 0.01$) and IL-2 (27.5%, IQR 18%–33%; $p < 0.01$) upon T cell activation with anti-CD3 and anti-CD28 than CD4$^+$ T cells from infant intestines (**Figures 3A and 3B**). Stimulation with phorbol 12-myristate 13- acetate and ionomycin (PMA-ionomycin) further augmented the production of TNF-α (64%, IQR 58%–70%; $p < 0.01$), IL-2 (73%, IQR 72%–85%; $p < 0.01$), and interferon-gamma (ifn-γ) (33.5%, IQR 24%–41%; $p < 0.01$) in fetal intestinal CD4$^+$ T cells compared with infant intestinal CD4$^+$ T cells (**Figures 3A and 3B**). Upon stimulation, the majority of fetal intestinal CD4$^+$ T cells expressed TNF-α in concert with IL-2 and, to a lesser extent, ifn-γ (**Figures 3A and 3C**). Analyses including only CD45R0$^+$CD4$^+$ T cells to account for differences in Tem populations demonstrated that also within CD45R0$^+$CD4$^+$ T cell populations, the frequencies of TNF-α$^+$CD4$^+$ T cells were higher in fetal than in infant intestines (**Figure S2A**). In line with the Th1 cytokine profile, T-box transcription factor TBX21 (T-BET) expression was high in fetal intestinal CD4$^+$ T cells (**Figure S2B**).

Treg cells have been described in fetal lymphoid nodes and were next investigated. Frequencies of fetal mesenteric-lymph node-derived Treg cells were similar to those in two previous studies (Michäelsson et al., 2006; Mold et al., 2008) (**Figures S2C and S2D**). However, in fetal intestinal lamina propria, CD127$^-$25$^+$CD4$^+$ Treg cells were scarce (5.5%, IQR 5.1%–10%) in comparison with Treg cells in infants (15.1%, IQR 9.6%–18.5%; $p < 0.05$), which was further confirmed by low expression of forkhead box P3 (FOXP3) by fetal CD4$^+$ T cells (**Figures 3D and 3E**). Upon stimulation, 1.6% (IQR 1.5%–3.6%) of infant intestinal CD4$^+$ T cells produced IL-10; however, IL-10 production was almost undetectable in fetal intestinal CD4$^+$ T cells ($p < 0.001$) (**Figure 3F**). t-SNE analyses showed that fetal intestinal Treg cells were not tissue resident (CD69$^-$), whereas CD69 was expressed by a proportion of infant intestinal Treg cells (**Figure S2E**). Overall, these data demonstrate that Treg cells are less frequent in the fetal intestine than in the infant intestine but increase later during development, as described previously (Thome et al., 2016). In addition, IL-4 production, which is characteristic of infant-blood-derived CD4$^+$ T cells (Zhang et al., 2014), did not differ significantly between fetal and infant intestinal CD4$^+$

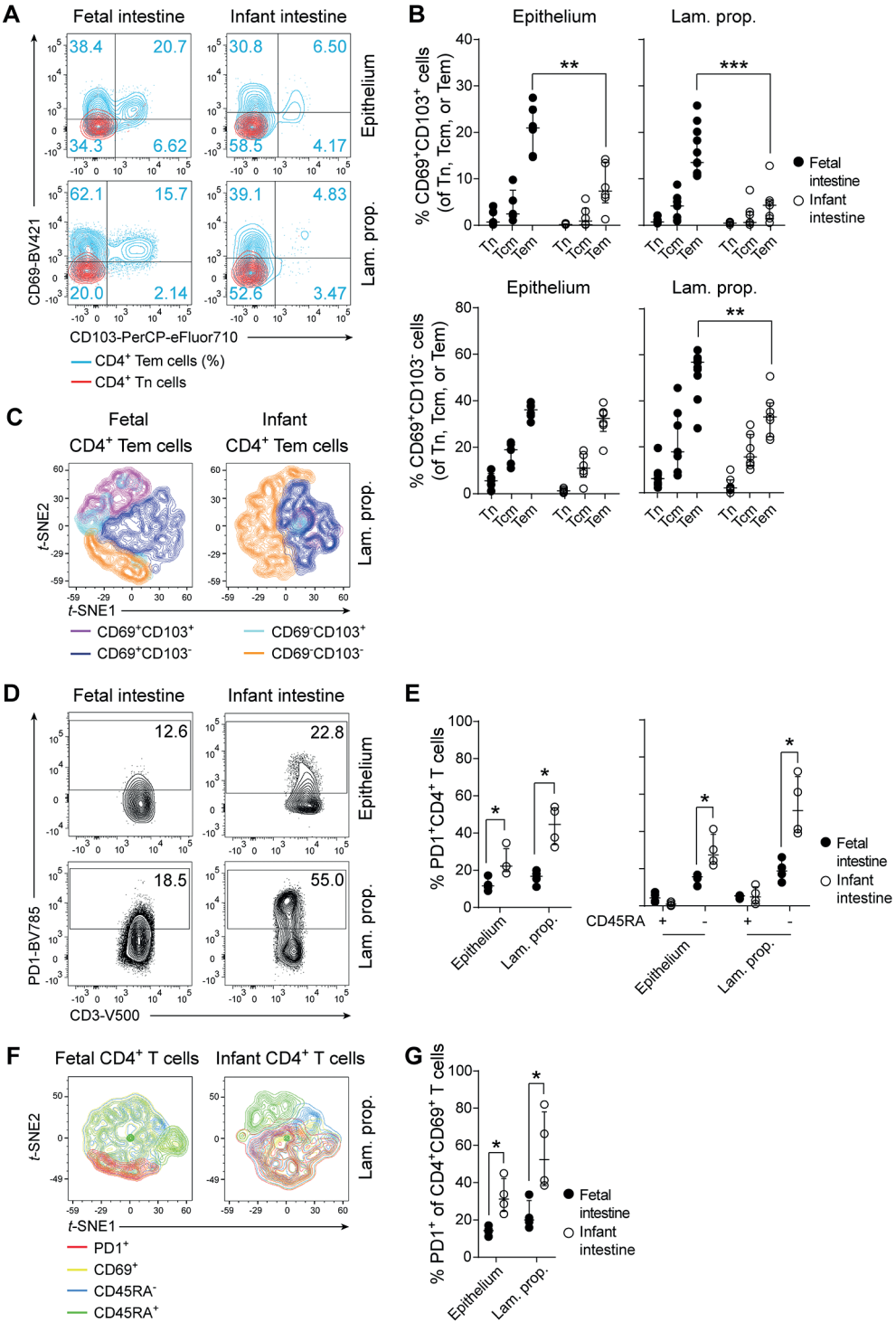
A
Fetal intestine
Infant intestine
38.4
20.7
34.3
6.62
30.8
6.50
58.5
4.17
62.1
15.7
20.0
2.14
39.1
4.83
52.6
3.47
Epithelium
Lam. prop.
CD69-BV421
CD103-PerCP-eFluor710
CD4+ Tem cells (%)
CD4+ Tn cells
B
Epithelium
Lam. prop.
% CD69+CD103+ cells (of Tn, Tcm, or Tem)
% CD69+CD103- cells (of Tn, Tcm, or Tem)
**
***
Tn
Tcm
Tem
Fetal intestine
Infant intestine
C
Fetal CD4+ Tem cells
Infant CD4+ Tem cells
t-SNE2
t-SNE1
Lam. prop.
CD69+CD103+
CD69+CD103-
CD69-CD103+
CD69-CD103-
D
Fetal intestine
Infant intestine
12.6
22.8
18.5
55.0
Epithelium
Lam. prop.
PD1-BV785
CD3-V500
E
% PD1+CD4+ T cells
*
Epithelium
Lam. prop.
CD45RA
+
-
Fetal intestine
Infant intestine
F
Fetal CD4+ T cells
Infant CD4+ T cells
t-SNE2
t-SNE1
Lam. prop.
PD1+
CD69+
CD45RA-
CD45RA+
G
% PD1+ of CD4+CD69+ T cells
Epithelium
Lam. prop.
Fetal intestine
Infant intestine

Figure 2. Fetal intestinal CD4+ Tem cells express CD69 and CD103 but limited PD1. (A) Flow-cytometric plots of CD69 and CD103 expression on fetal and infant CD4+ Tn (red) and Tem (blue; percentages) cells in epithelium and lamina propria intestinal tissues. (B) Median percentage (±IQR) of CD69+103+ (top two graphs) and CD69+103- (bottom two graphs) of fetal or infant epithelium- and lamina-propria-derived CD4+ Tn, Tcm, or Tem cells. Shown are fetal epithelium (n = 6) and lamina propria (n = 11) samples and infant epithelium (n = 6) and lamina propria (n = 7) samples. (C) t-SNE plot of CD69 and CD103 expression on fetal and infant lamina-propria-derived CD4+ Tem cells. (D) Flow-cytometric plots of PD1 expression on fetal and infant epithelium- and lamina-propria-derived CD4+ T cells. (E) Median percentage (±IQR) of PD1+ fetal and infant epithelium- and lamina-propria-derived CD4+ T cells (left) and CD45RA+ or CD45RA-CD4+ T cell subsets (right). Shown are fetal epithelium (n = 4) and lamina propria (n = 4) samples and infant epithelium (n = 4) and lamina propria (n = 4) samples. (F) t-SNE plot of PD1, CD69, and CD45RA expression on fetal and infant lamina-propria-derived CD4+ T cells. (G) Median percentage (±IQR) of fetal and infant epithelium- and lamina-propria-derived PD1+ cells of CD4+CD69+ T cells. Shown are fetal epithelium (n = 4) and lamina propria (n = 4) samples and infant epithelium (n = 4) and lamina propria (n = 4) samples. Statistical significance was measured by Mann-Whitney U comparisons. *p < 0.05, **p < 0.01, ***p < 0.001. Abbreviations are as follows: lam. prop., lamina propria; Tn, naive T cells; and Tem, effector memory T cells.

T cells (**Figure 3F**). Also, CXCL8 production did not differ between intestinal fetal and infant CD4+ T cells (**Figure S3A**). Furthermore, fetal intestinal CD4+ T cells did not produce IL-17A upon stimulation, whereas 4.6% (IQR 2.8%–7.3%) of infant CD4+ T cells produced IL-17A upon PMA-ionomycin stimulation ($p < 0.01$) (**Figure S3B**). IL-22 was produced by a small number of fetal and infant intestinal CD4+ T cells (**Figure S3C**). Altogether, these data demonstrate that TNF-α-producing CD4+ T cells are the predominant subtype in fetal intestines.

Transcriptome of single fetal intestinal CD4+ T cells is characterized by genes mediating Th1 cells and growth

Fetal and infant intestinal CD4+ T cells differ on the basis of predefined markers in T cell biology. scRNA-seq is an unbiased approach to identifying unique transcriptomic signatures on the single-cell level (Grün and van Oudenaarden, 2015; Tang et al., 2009). In total, scRNA-seq data of 2,147 fetal intestinal T cells from 2 donors and 754 infant intestinal CD4+ T cells from 4 donors were obtained. The purity of the sorted intestinal CD4+ T cells was confirmed by the low expression of genes expressed by parenchymal intestinal epithelial cells (**Figure S4A**). Unstimulated fetal and infant intestinal CD4+ T cells formed separate clusters (**Figure 4A**). A further separation of epithelium and lamina-propria-derived CD4+ T cells was observed for fetal cells (**Figure 4A**). Gene-set enrichment analysis showed clustering of related Gene Ontology (GO) terms in unstimulated fetal intestinal CD4+ T cells (**Figure 4B**). One of the largest clusters included GO terms related to T cell activation. Large clusters also included GOterms related to the cell cycle, wingless-related integration site (WNT) signaling, and mitogen-activated protein kinase (MAPK) signaling (**Figure 4B**). Next, we determined the GO terms that significantly differed between stimulated fetal and infant intestinal CD4+ T cells. Stimulated fetal and infant intestinal CD4+ T cells clustered separately; a more homogeneous fetal cell cluster and individual infant clusters indicated higher heterogeneity among infant cell populations (**Figure 4C**).

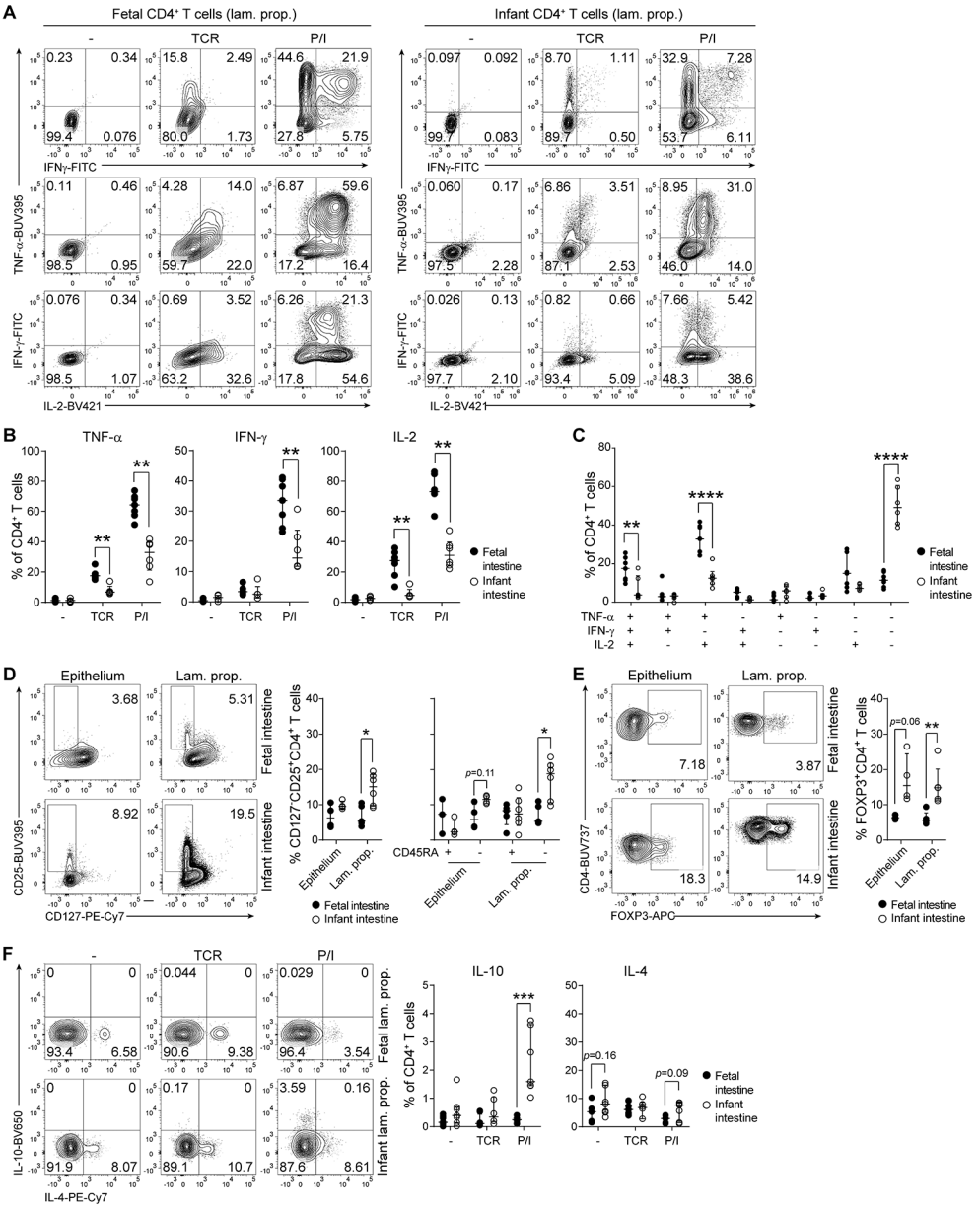

Figure 3. Fetal intestinal CD4⁺ T Cells produce TNF-α, IFN-γ, and IL-2, whereas Treg cells are scarce. (A) Flow-cytometric plots of TNF-α, IFN-γ, and IL-2 expression in unstimulated or stimulated (with anti-CD3 and anti-CD28 [TCR] or PMA-ionomycine [P/I]) lamina-propria-derived CD4⁺ T cells from fetal (left) and infant (right) intestines. (B) Median percentage (±IQR) of TNF-α⁺, IFN-γ⁺, or IL-2⁺ lamina-propria-derived CD4⁺ T cells unstimulated or stimulated with TCR or P/I. Shown are fetal lamina propria-derived CD4⁺ T cells in unstimulated conditions (n = 6) and TCR and P/I conditions (n = 7) and infant lamina-propria-derived CD4⁺ T cells in unstimulated and P/I conditions (n = 6) and TCR conditions (n = 5). (C) Median percentage (±IQR) of lamina-propria-derived CD4⁺ T cells co-expressing TNF-α, IFN-γ, and IL-2 in fetal and infant intestines upon P/I stimulations. Shown are fetal (n = 7) and infant (n = 6) lamina- ▸

propria-derived CD4+ T cells (D) Flow-cytometric plots of CD127-CD25+ CD4+ Treg cells in fetal and infant epithelium and lamina propria intestinal samples (left) and median percentages (±IQR) of CD127-CD25+ cells of total intestinal CD4+ T cells and intestinal CD45RA+ or CD45RA-CD4+ T cells (right). Shown are fetal epithelium (n = 4) and lamina propria (n = 5) samples and infant epithelium (n = 4) and lamina propria (n = 6) samples. (E) Flow-cytometric plots (left) and median percentages (±IQR) of FOXP3+CD4+ Treg cells in fetal and infant intestinal epithelium and lamina propria intestinal samples (right). Shown are fetal epithelium (n = 3) and lamina propria (n = 5) samples and infant epithelium (n = 4) and lamina propria (n = 5) samples. (F) Flow-cytometric plots (left) and median percentages (±IQR) of unstimulated and stimulated (with TCR or P/I) lamina-propria-derived IL-10+ and IL-4+ CD4+ T cells (right). Shown are fetal CD4+ T cells in unstimulated and TCR conditions (n = 7) and P/I conditions (n = 8) and infant CD4+ T cells in unstimulated and P/I conditions (n = 7) and TCR conditions (n = 6). Statistical significance was measured by Mann-Whitney U comparisons or (C) ANOVA with Bonferroni's correction for multiple comparisons. *p < 0.05, **p < 0.01, ***p < 0.01, ****p < 0.0001. Abbreviations are as follows: lam. prop., lamina propria; TCR, anti-CD3 and anti-CD28; and P/I, PMA-ionomycin. See **Figures S2, S3, and S6**.

The expression of genes in GO terms summarizing nuclear factor kappa-light-chain-enhancer of activated B cells (NF-κB) signaling, as well as genes in GO terms of IL-12-mediated signaling, was significantly increased in stimulated fetal compared with infant intestinal CD4+ Tem cells (**Figure 4D**). NF-kB, together with IL-12, mediates the differentiation of Th1 cells (Aronica et al., 1999; Athie-Morales et al., 2004; Hilliard et al., 2002). Furthermore, genes in the GO term regulation of epithelium morphogenesis were significantly upregulated in stimulated fetal intestinal CD4+ Tem cells, which was in line with the GO terms defining fetal intestinal T cells at baseline (**Figure 4D**). Altogether, these single-cell analyses of fetal intestinal CD4+ T cells showed a gene profile associated with Th1 cell differentiation and epithelial growth.

Next, we investigated individual genes differentially expressed by stimulated fetal and infant CD4+ Tem cells. Consistent with the GO term analyses, stimulated fetal intestinal CD4+ Tem cells strongly expressed genes encoding proteins involved in the NF-κB pathway (*NFKB1* and *NFKBIA*) (**Figures 4E and S4B**). Furthermore, genes encoding Th1-type cytokines and chemokines (*IFNG* and *IL2*, as well as *CXCL1* and *XCL2*) were significantly upregulated in fetal intestinal CD4+ Tem cells compared with infant cells. *TNF* mRNA, however, was not differentially expressed between fetal and infant intestinal CD4+ Tem cells. TNF-α production is strongly dependent on post-transcriptional regulation by several other proteins, in particular MAP-kinase activated protein kinase 2 (MAPKAP2) (Brook et al., 2000; Kotlyarov et al., 1999), and *MAPKAP2* mRNA was significantly upregulated in fetal intestinal CD4+ Tem cells compared with infant cells (**Figures 4E and S4B**), most likely allowing for the increased protein detected in fetal intestinal CD4+ T cells. GO terms representing the MAPK cascade were also already dominantly present in the unstimulated fetal intestinal CD4+ T cells (**Figure 4B**). Next to the Th1 cell phenotype, fetal CD4+ T cells were further characterized by GO terms summarizing genes involved in the cell cycle and tissue development. In line with this, genes encoding proteins involved in regulating the cell cycle (such as *PTMA* and *SET*; Eilers et al., 1991; Fan et al., 2003) and encoding proteins involved in transcription factor networks mediating tissue and T cell development (such as *HSPA8* and *NACA*; Lehtinen et al., 2006; Mendillo et al., 2012) were expressed significantly more in stimulated fetal than in infant intestinal CD4+ Tem cells. Lastly, genes regulating cell

metabolism and promoting cell growth (*ENO1*, *ODC1*, *NAMPT*, *PFKP*, and *STK4* [Auvinen et al., 1992; Gerner et al., 2018; Meienhofer et al., 1979; Stefanini, 1972; Abdollahpour et al., 2012]) were significantly upregulated in fetal compared with infant stimulated intestinal CD4⁺ T cells. Altogether, these scRNA-seq data demonstrate that fetal intestinal CD4⁺ T cells exhibit enhanced production of Th1-cell-related cytokines, supporting our data obtained by multi-parameter flow cytometry. Furthermore, genes involved in the cell cycle and tissue growth were

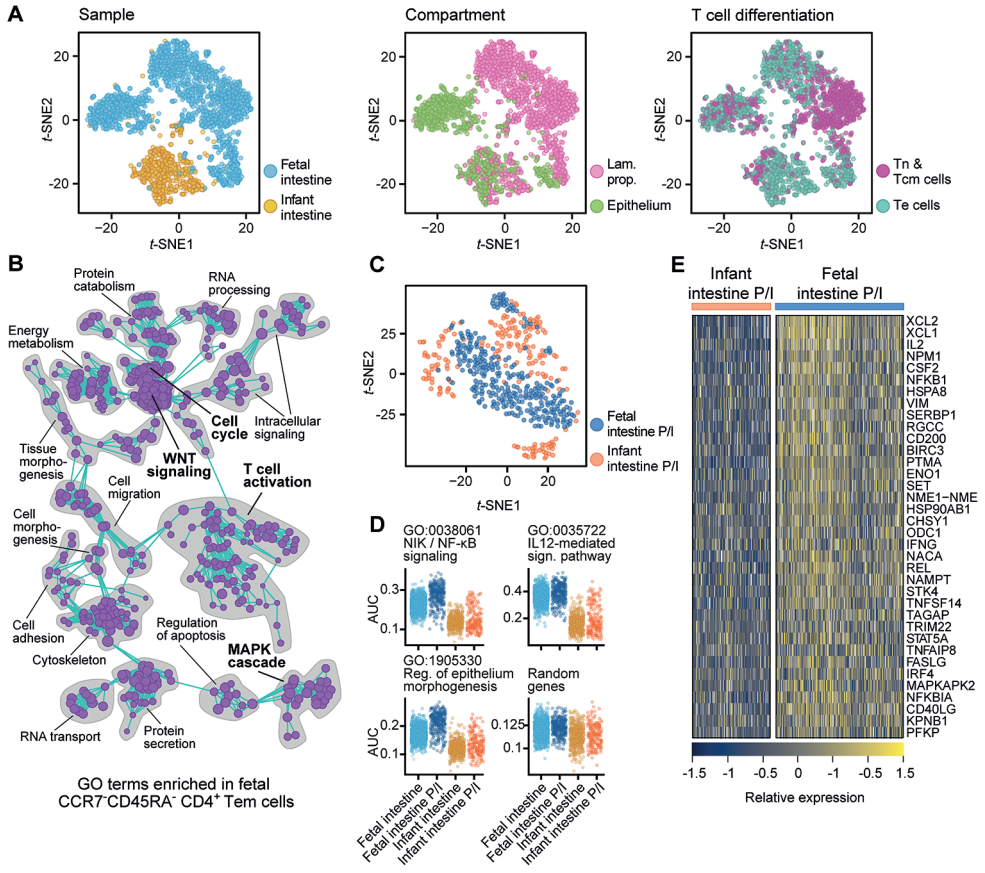

Figure 4. Transcriptome of fetal intestinal CD4⁺ T cells is characterized by genes mediating Th1 cells and growth. (A) t-SNE plots of unstimulated intestinal CD4⁺ T cells indicating fetal and infant samples (left), tissue compartment (middle), or T cell subset (right). (B) Gene Ontology (GO) term map showing a network of GO terms enriched in fetal CD4⁺ Tem cells. (C) t-SNE plot of gene expression in fetal and infant P/I-stimulated CD4⁺ Tem cells. (D) Enrichment of selected GO term signatures plotted individually for all stimulated intestinal CD4⁺ Tem cells as the area under the curve (AUC) of a recovery curve of expression-sorted genes. (E) Heatmap of genes significantly upregulated in fetal compared with infant P/I-stimulated intestinal CD4⁺ Tem cells. Abbreviations are as follows: Tem, effector memory T cells; Tcm, central memory T cells; Tn, naive T cells; lam. prop., lamina propria; P/I, PMA-ionomycin; GO, Gene Ontology; AUC, area under the curve; sign., signaling; and reg., regulation. Sample sizes are as follows: fetal epithelium, n = 2; fetal lam. prop., n = 2; infant epithelium, n = 4; and infant lam. prop., n = 4. See **Figure S4**.

significantly upregulated in fetal intestinal CD4+ T cells, indicating a unique T cell phenotype in fetal intestines and pointing toward a potential role in tissue development.

TNF-α has a dose-dependent effect on fetal ISC development

The lamina propria envelopes ISCs in the crypts, allowing close contact between lamina-propria-derived CD4+ T cells and ISCs, whereas epithelial CD4+ T cells are positioned between the intestinal epithelial cells (Bunders et al., 2012). The effect of TNF-α, the predominant cytokine produced by fetal intestinal CD4+ T cells, on intestinal development was assessed in ISC organoid cultures. ISCs from fetal intestinal tissues were isolated and seeded to grow into organoids (Sato and Clevers, 2013). Cells from organoids strongly expressed leucine-rich-repeat containing G-protein-coupled receptor (*LGR5*) mRNA, verifying the presence of ISCs in fetal intestinal epithelium-derived organoids (**Figure S5A**). Furthermore, we confirmed expression of mRNA of TNF-α receptors (*TNFRSF1A* and *TNFRSF1B*) by fetal ISCs (**Figure S5B**). Next, the effect of TNF-α on fetal ISCs in *in vitro* organoid systems was determined. In cultures with 0.2 ng/mL TNF-α, the numbers of organoids were significantly higher than in control cultures without TNF-α (**Figures 5A and 5B**). In contrast, TNF-α concentrations R 20 ng/mL reduced the number of developing organoids and impaired ISC proliferation (**Figures 5A and 5B**), in line with the described role of high concentrations of TNF-α in inducing apoptosis (Begue et al., 2006; Sands and Kaplan, 2007). WNT signaling is critical for the proliferation of stem cells (Kretzschmar and Clevers, 2017), and NF-kB can further enhance WNT signaling and upregulate expression of WNT target genes (Schwitalla et al., 2013), promoting ISC proliferation. Whole-genome RNA sequencing of fetal ISCs stimulated with different concentrations of TNF-α showed that the expression of previously identified targets of WNT signaling, such as *ASCL2* and *FSTL1* (van der Flier et al., 2009; Schwitalla et al., 2013), was high in ISC cultures at low concentrations of TNF-α and decreased with increasing TNF-α concentration (**Figure S5C**). Organoid cultures with high TNF-α concentrations furthermore exhibited increased expression of genes mediating apoptosis, such as *FOXO1* and *TNFSF10* (**Figure S5D**). Together, these data show that TNF-α has a dose-dependent effect on fetal ISC development whereby low concentrations support ISC growth and high concentrations of TNF-α prevent ISC proliferation.Next, we determined the direct impact of fetal intestinal CD4+ T cells on ISC growth. To this end, *in vitro* co-culture systems of intestinal CD4+ Tem cells with ISCs were developed. ISCs were seeded together with sorted and then activated (anti-CD3 and anti-CD28) fetal intestinal (lamina-propria-derived) CD4+ Tem cells in either a low (30 cells per µL Matrigel) or high (800 cells per µL Matrigel) concentration. Low numbers of fetal intestinal CD4+ Tem cells promoted organoid outgrowth, resulting in the tripling of organoids (**Figures 5C and 5D**). TNF-α blockade abolished fetal-T-cell-mediated enhanced organoid outgrowth, demonstrating that this process was TNF-α dependent (**Figures 5C and 5D**). In contrast, high fetal T cell numbers impeded ISC proliferation, indicating an inhibitory effect of fetal intestinal CD4+ T cells (**Figures 5E and 5F**). This inhibitory effect of high numbers of fetal intestinal CD4+ T cells was again TNF-α dependent given that TNF-α blockade restored ISC outgrowth and organoid numbers. Collectively, these *in vitro* data from intestinal CD4+ T cell and ISC co-culture systems

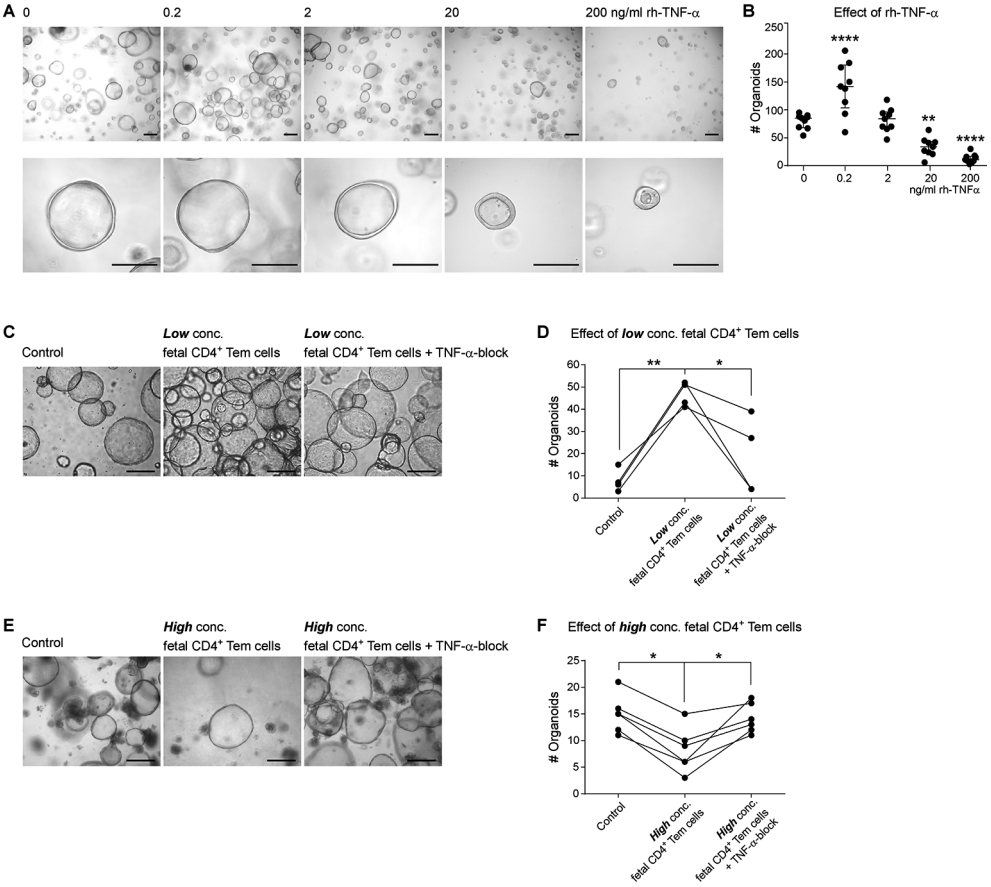

Figure 5. Fetal intestinal CD4⁺ Tem cells have a dose-dependent effect on intestinal stem cell development. (A) Fetal intestinal organoid cultures with increasing concentrations of recombinant human (rh) TNF-α. (B) Median number (±IQR) of fetal organoids per drop. Data represent one donor and were replicated in two additional donors. (C) Fetal intestinal organoid cultures with medium (control) co-cultured with a low concentration (30 cells per 1 µL Matrigel) of fetal CD4⁺ Tem cells and co-cultured with a low concentration of fetal CD4⁺ Tem cells and TNF-α block. (D) Number (±IQR) of fetal organoids per field of view (FOV) (two fetal tissue donors). (E) Fetal intestinal organoid cultures with normal medium (control) co-cultured with a high concentration (800 cells per 1 µL Matrigel) of fetal lamina-propria-derived CD4⁺ Tem cells and co-cultured with a high concentration of fetal lamina-propria-derived CD4⁺ Tem cells and TNF-α block. (F) Number (±IQR) of fetal organoids per FOV (two fetal tissue donors). Statistical significance was measured with one-way ANOVA with Bonferroni's correction for multiple comparisons (B), comparing all conditions to 0 ng rh-TNF-α/mL, and (D and F) Mann-Whitney U comparisons. *$p < 0.05$, **$p < 0.01$, ****$p < 0.0001$. Abbreviations are as follows: rh, recombinant human; ISC, intestinal stem cell; conc., concentration; Tem, effector memory T cell; and FOV, field of view. Black scale bars represent 200 mm. See **Figure S5**.

show that intestinal fetal CD4⁺ Tem cells have a dose-dependent and TNF-α-mediated effect on ISC proliferation; this effect supports intestinal epithelial growth and development under physiological conditions but can prevent epithelial growth at high concentrations.

Inflamed intestines of preterm infants show an enhanced TNF-α signature

Preterm infants are at risk of developing intestinal inflammation that can lead to NEC (Neu and Walker, 2011). Our studies show that early in human development TNF-α-producing CD4+ T cells are preferentially present in fetal intestines and can support intestinal development but that high concentrations of TNF-α can also inhibit epithelial growth *in vitro*. We hypothesized that preterm birth and antigen exposure can result in further activation and recruitment of TNF-α-producing CD4+ Tem cells in NEC, whereas preterm infants without NEC would have a phenotype resembling CD4+ T cells in older children. In comparison with fetal tissues, tissues from infants with NEC showed large numbers of T cells in the epithelium and lamina propria of NEC-affected tissues (**Figure 6A**). We further isolated cells from the intestinal tissues of six preterm infants with NEC (median 25 weeks of gestation at birth; median age 9.5 days at surgery) and observed that 57% (median, IQR 49%–60%) of CD3+ T cells were CD4+8- T cells. The frequencies of naive CD4+ T cells were significantly lower in the inflamed intestines of preterm infants with NEC and showed a more differentiated phenotype than intestinal CD4+ T cells derived from preterm infants without intestinal inflammation or infants born at term (**Figures 6B and 6C**). Intestinal CD4+ T cells derived from NEC tissues produced TNF-α already at baseline, and this was further upregulated upon stimulation with PMA-ionomycin (**Figures S6A and 6D**), whereas IL-10 production by CD4+ T cells from NEC tissues was absent (**Figures 6D and 6E**). Overall, these data show that CD4+ T cells in inflamed intestinal tissue of preterm infants with NEC had an effector memory phenotype with preferential TNF-α production. To determine whether TNF-α and genes downstream of TNF signaling were expressed in NEC tissues, we quantified mRNA expression in NEC tissues. The mRNA of the genes *TNFA*, *NFKBIA*, *TNFAIP2*, and *TNFAIP3* was significantly enhanced in tissues derived from NEC patients compared with infants born at term, consistent with higher TNF-α signaling (**Figure 6F**). *Ex vivo* analyses of fetal intestinal tissues without inflammation showed a trend toward higher *NFKBIA* and *TNFAIP3* expression than in intestines from infants born at term (**Figure 6F**), consistent with the observed TNF-α production *ex vivo*. Together, these data show that CD4+ Tem cells were increased in NEC tissues and preferentially produced TNF-α. Furthermore, a gene expression signature consistent with enhanced TNF-α signaling was observed in intestinal tissues from preterm infants with NEC.

DISCUSSION

The fetal immune system is traditionally characterized as tolerogenic (McGovern et al., 2017; Michäelsson et al., 2006; Mold et al., 2008). Here, we demonstrated that early in human development clonally expanded TNF-α-producing CD4+ Tem cells were present in fetal intestines, whereas Treg cells were scarce, indicating early compartmentalization of immune responses. Fetal intestinal CD4+ Tem cell populations produced TNF-α and supported intestinal development in ISC and T cell co-cultures. In contrast, high numbers of intestinal TNF-α+CD4+ T cells impaired intestinal development. This was in line with *in vivo* observations in premature NEC-affected infants, in whom we observed infiltration with TNF-α+CD4+ Tem cells and a TNF-

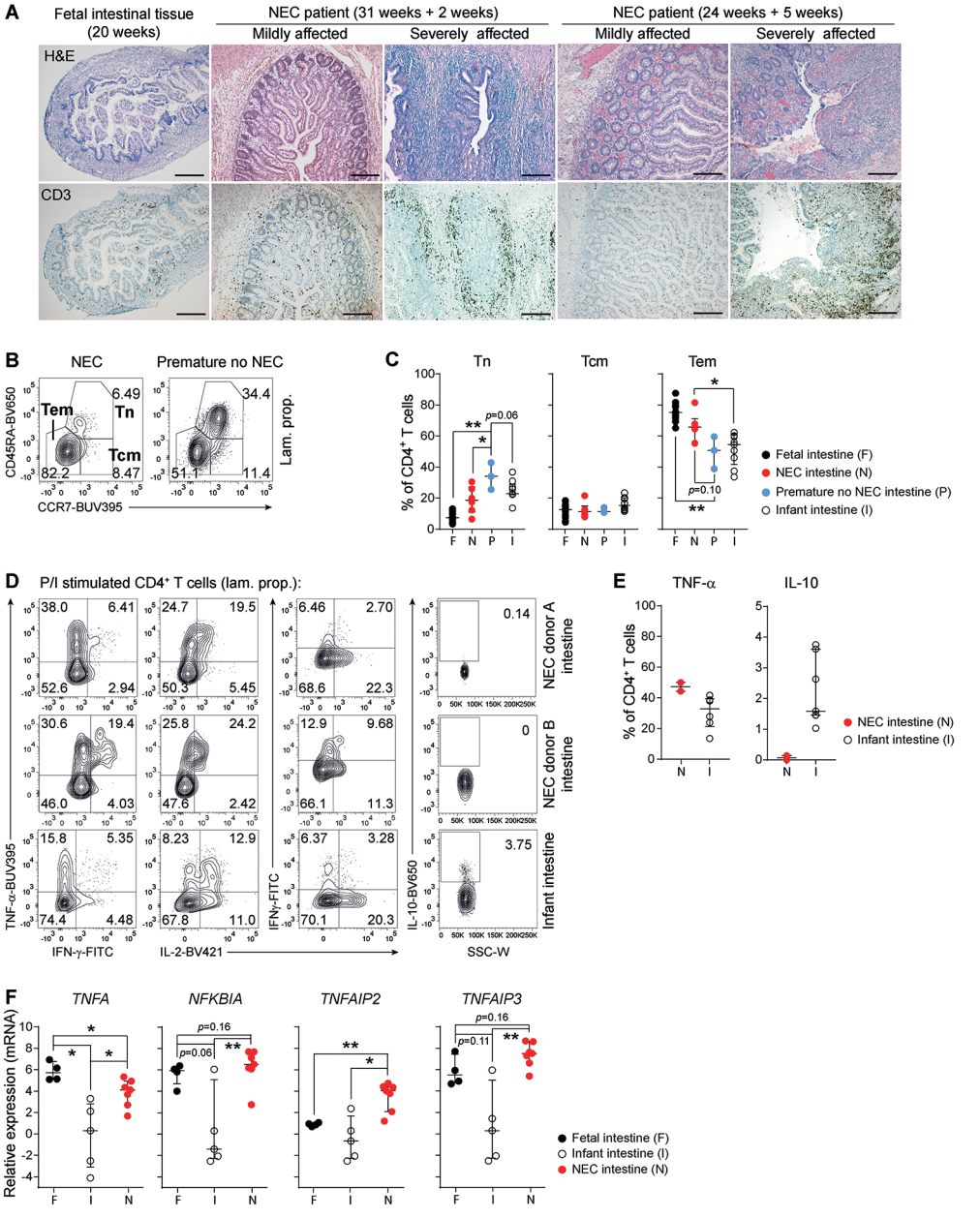

Figure 6. CD4⁺ T cells in NEC intestinal tissue show a TNF gene profile. (A) Images of immunohistochemical analyses of fetal intestine and two representative NEC tissues of seven NEC tissues analyzed. A mildly affected tissue segment and a severely affected tissue segment of the same NEC donors are shown. Stainings are with hematoxylin and eosin and DAB for T cells (CD3) (brown; cell nuclei in blue). (B) Flow-cytometric plots of CD45RA and CCR7 expression on lamina-propria-derived CD4⁺ T cells from one NEC patient and one premature infant without NEC. (C) Median percentage (±IQR) of lamina-propria-derived CD4⁺ T cell subsets (left to right) CD45RA⁺CCR7⁺ Tn, CD45RA⁻CCR7⁺ Tcm, and CD45RA⁻CCR7⁻ Tem in fetal (F) (n = 13), NEC (N) (n = 6), non-NEC premature infant (P) (n = 3) intestines, and intestines of term infants ▸

(I) (n = 9). (D) Flow-cytometric plots of expression of TNF-α, IFN-γ, and IL-2 in PMA-ionomycine (P/I)-stimulated lamina-propria-derived CD4+ T cells from two NEC-affected intestines (top two rows) and the intestine of one term infant (bottom row). (E) Median percentages (±IQR) of P/I-stimulated lamina-propria-derived TNF-α+ or IL-10+ CD4+ T cells from NEC tissues or intestines of term infants. (F) Median relative mRNA expression (log2) (±IQR) of *TNFA*, *NFKBIA*, *TNFAIP2*, and *TNFAIP3* in NEC (N) tissues (n = 7) compared with non-inflamed fetal (F) (n = 4) and infant (I) (n = 5) tissues. Statistical significance was measured by Mann-Whitney U comparisons. *p < 0.05, **p < 0.01. Black scale bars represent 200 mm. Abbreviations are as follows: lam. prop., lamina propria; Tn, naive T cell; Tcm, central memory T cell; Tem, effector memory T cell; P/I, PMA-ionomycin. See **Figure S6**.

induced gene expression profile in the inflamed intestines. These data support a model in which human fetal intestinal CD4+ T cells can mediate tissue development, whereas dysregulation of this process resulting from preterm birth and premature exposure to antigens can contribute to intestinal inflammation because regulatory mechanisms are not yet in place. The results from these studies of intestinal development in humans further challenge a solely tolerogenic model of immune ontogeny early in life.

Previous studies of infant blood have shown a predominance of Th2- and Treg-cell-biased responses (Michäelsson et al., 2006; Prendergast et al., 2012; Zhang et al., 2014). Recently, Mc-Govern et al. (2017) provided a mechanism for this tolerogenic immune status by demonstrating that enhanced arginase-2 activity in fetal DCs derived from spleens promoted the induction of Treg cells and diminished TNF-α production by T cells. The authors also showed that fetal intestines harbored predominantly classical DC1s (cDC1s), which can induce Th1 responses, rather than tolerance-inducing splenic classical cDC2s. IL-12 production by DCs is critical for the polarization toward Th1 cells (Athie-Morales et al., 2004), and fetal intestinal CD4+ T cells indeed showed upregulation of genes mediated by IL-12 signaling. The presence of cDC1s appears to be unique to fetal intestines given that cDC2s are prevalent in infant and adult intestines (Granot et al., 2017). The data presented here demonstrate a predominance of TNF-α-producing CD4+ T cells in intestines of fetuses with a Th1 cell transcriptomics profile, whereas a broadened intestinal CD4+ T cell repertoire, including functional Treg cells, was observed in infants. Intestines of preterm infants born at the beginning of the third trimester without intestinal inflammation harbored an increased number of naive CD4+ T cells, suggesting that substantial modifications occur at this time. Tissue-specific compartmentalization of human CD4+ T cells allows fetal CD4+ T cells to have functional differences that can be tailored toward the specific requirements of the respective tissues at that particular developmental stage, such as TNF-α-producing CD4+ T cells in the intestine of fetuses and predominantly Treg and Th2 cell responses in the blood to enable maternal-fetal equilibrium during pregnancy. The memory features of fetal intestinal CD4+ Tem cells, including *IRF4* expression and clonal expansion, suggest a TCR-triggered memory induction rather than a memory-like induction in a lymphopenic environment (Le Saout et al., 2008). However, the origins of the antigens responsible remain elusive and might include maternal antigens (Mold et al., 2008), autoantigens, or even antigens derived from microbes passing through the placenta (Collado et al., 2016). Further studies are needed to answer these fundamental questions.

During the second trimester of gestation, corresponding to the time at which fetal tissues were investigated in this study, fetal intestinal growth accelerates to peak velocity (Weaver et al., 1991). Inflammation is generally perceived to be disadvantageous during fetal development, and in utero infections that trigger immune responses are associated with impaired fetal growth (Mor et al., 2017). However, immune cells have been recently recognized for their role in tissue regeneration of the intestinal epithelium after tissue damage (Lindemans et al., 2015).

Here, we demonstrated that fetal intestinal $CD4^+$ T cells by means of TNF-α at relatively low concentrations promoted the outgrowth of fetal ISCs, revealing a supportive role of TNF-α produced by T cells in mucosal development prior to birth. TNF-α has been shown to facilitate tumor growth (Orosz et al., 1993) through NF-κB enhancement of WNT signaling (Schwitalla et al., 2013). Human fetal cells from other tissues, such as microglial cells, also exhibit TNF-α-biased cytokine production (Chao et al., 1995; Zolti et al., 1991), suggesting a shared pathway in development. In contrast to humans, fetal mice did not have T cells in the intestinal mucosa, and murine fetal intestinal stem cells can produce endogenous growth factors, rendering them less dependent on exogenously produced factors (Nusse et al., 2018). Furthermore, TNF-deficient mice have normal epithelial development under homeostatic conditions (Kuprash et al., 2005). The data presented here emphasize the importance of human studies of immune ontogeny. Using scRNA-seq analyses of intestinal T cell populations, we observed that, compared with infant intestinal $CD4^+$ T cells, fetal intestinal $CD4^+$ T cells had a distinctive gene expression profile characterized by high expression of genes regulating cell cycle, WNT signaling, and tissue development. Although we did not detect enhanced expression of *TNF* in fetal intestinal $CD4^+$ T cells, we observed significantly higher expression of *MAPKAPK2* and other genes related to MAPK signaling and involved in post-transcriptional regulation of TNF-α (Kotlyarov et al., 1999), suggesting that elevated TNF-α by fetal compared with infant intestinal $CD4^+$ T cells might result from post-transcriptional regulation. Overall, these data indicate that $CD4^+$ T cells in fetal intestines can promote tissue development and support the emerging concept that fetal growth represents a highly controlled process in which immune cells support tissue generation.

High concentrations of TNF-α and numbers of TNF-α^+CD4^+ T cells impaired ISC growth. This TNF-α-mediated detrimental effect on intestinal tissue development is in line with observations from *ex vivo* analyses of intestinal tissues from premature infants with NEC, demonstrating that $CD4^+$ T cells are increased in intestines of preterm infants with NEC and produce TNF-α. Whereas the intestinal $CD4^+$ T cell compartment in preterm infants with NEC resembled fetal intestines, intestines of preterm infants without NEC largely harbored naive $CD4^+$ T cells, reflective of observations in older infants. Furthermore, intestinal tissues of infants with NEC showed high expression of genes upregulated in response to TNF-α signaling, revealing a TNF-α footprint in NEC tissues. Thus, peak incidence of NEC occurs at a time during human immune development when dramatic changes in immune cell populations take place. The high susceptibility of prematurely born infants to NEC might be furthermore enhanced by limited immune regulatory properties. PD1 was low in fetal compared with infant intestinal $CD4^+$ T cells, and IL-10^+ Treg cells were scarce in fetal intestines, as well as in NEC samples, the latter of which is in line with previous data (Weitkamp et al., 2013). Because of

the lack of appropriate animal models and the unfeasibility of longitudinal samples obtained before and during NEC in infants, it is difficult to unequivocally determine causes and effects of TNF-α+CD4+ T cells in NEC. However, the data presented in this study suggest a model in which, depending on the individual maturation status of the intestinal T cell compartment in the infant at the time of preterm birth, premature exposure to the external environment can result in intestinal inflammation and NEC. Further studies are needed to determine whether anti-TNF treatments that are successfully used in inflammatory bowel diseases in adults (Sands and Kaplan, 2007) also represent a therapeutic option in NEC.

In conclusion, our findings provide a new framework for intestinal immune ontogeny in which intestinal CD4+ Tem cells can support mucosal development prior to birth in the in utero environment and reconcile our fundamental understanding of early life human T cell responses with the increased risk of intestinal inflammation in preterm infants.

STAR METHODS

A more detailed version of the methods are provided in the online version of this paper.

SUPPLEMENTAL INFORMATION

Supplemental Information includes six figures and one table.

ACKNOWLEDGMENTS

The authors would like to thank Dr. Weijer, Dr. Voordouw, and the Bloemenhove clinic (Heemstede, the Netherlands) for collecting and providing fetal tissues; Dr. Remmerswaal, Dr. Hooijbrink, and Mr. D€usedau for assistance in flow-cytometric analyses; and Dr. Dijkstra-Muncan and Ms. Martins Garcia for assistance in organoid experiments. We thank the Utrecht Sequencing Facility for providing sequencing service. The Utrecht Sequencing Facility is subsidized by the University Medical Center Utrecht, Hubrecht Institute, and Utrecht University. This work was supported by the Dutch Digestive Fund (MLDS Project CDG 15-02), the Deutsche Forschungsgemeinschaft (DFG; SFB841), the Stichting Steun Emma (WAR008-2015-03-002), and the Daisy Hüet Röell Foundation.

AUTHOR CONTRIBUTIONS

M.J.B. and R.R.C.E.S. designed the experiments. M.E.B., A.F.S., N.S., F.L.S., A.D., and S.-M.M.L.T. contributed to experiments; R.B., J.P.M.D., and K.R. collected samples; M.K. and M.A.F. analyzed single-cell data; M.M., S.M., and E.E.S.N. contributed to the design of the organoid sequencing experiments; J.M.v.R. and M.J.B. performed the organoid sequencing experiments; S.T.P. performed the IHC experiments; N.S. and N.G. performed mice experiments; P.L.K. and N.d.V. performed TCR sequencing; T.B.H.G., E.E.S.N., and J.B.v.G. contributed to the study

design, interpretation of the data, and manuscript revision; R.R.C.E.S. performed the data analyses; R.R.C.E.S. and M.J.B. wrote the manuscript with input from all authors; and M.J.B. supervised the study.

DECLARATION OF INTERESTS

The authors declare no competing interests.

REFERENCES

Abdollahpour, H., Appaswamy, G., Kotlarz, D., Diestelhorst, J., Beier, R., Sch€affer, A.A., Gertz, E.M., Schambach, A., Kreipe, H.H., Pfeifer, D., et al. (2012). The phenotype of human STK4 deficiency. Blood 119, 3450–3457.

Aibar, S., Gonza´ lez-Blas, C.B., Moerman, T., Huynh-Thu, V.A., Imrichova, H., Hulselmans, G., Rambow, F., Marine, J.C., Geurts, P., Aerts, J., et al. (2017). SCENIC: single-cell regulatory network inference and clustering. Nat. Methods 14, 1083–1086.

Aronica, M.A., Mora, A.L., Mitchell, D.B., Finn, P.W., Johnson, J.E., Sheller, J.R., and Boothby, M.R. (1999). Preferential role for NF-k B/Rel signaling in the type 1 but not type 2 T cell-dependent immune response in vivo. J. Immunol. 163, 5116–5124.

Athie-Morales, V., Smits, H.H., Cantrell, D.A., and Hilkens, C.M.U. (2004). Sustained IL-12 signaling is required for Th1 development. J. Immunol. 172, 61–69.

Auvinen, M., Paasinen, A., Andersson, L.C., and Hölttä, E. (1992). Ornithine decarboxylase activity is critical for cell transformation. Nature 360, 355–358.

Begue, B., Wajant, H., Bambou, J.C., Dubuquoy, L., Siegmund, D., Beaulieu, J.F., Canioni, D., Berrebi, D., Brousse, N., Desreumaux, P., et al. (2006).

Implication of TNF-related apoptosis-inducing ligand in inflammatory intestinal epithelial lesions. Gastroenterology 130, 1962–1974.

Brook, M., Sully, G., Clark, A.R., and Saklatvala, J. (2000). Regulation of tumour necrosis factor alpha mRNA stability by the mitogen-activated protein kinase p38 signalling cascade. FEBS Lett. 483, 57–61.

Bunders, M.J., van der Loos, C.M., Klarenbeek, P.L., van Hamme, J.L., Boer, K., Wilde, J.C.H., de Vries, N., van Lier, R.A., Kootstra, N., Pals, S.T., and Kuijpers, T.W. (2012). Memory CD4(+)CCR5(+) T cells are abundantly present in the gut of newborn infants to facilitate mother-to-child transmission of HIV-1. Blood. 120, 4383–4390.

Butler, A., Hoffman, P., Smibert, P., Papalexi, E., and Satija, R. (2018). Integrating single-cell transcriptomic data across different conditions, technologies, and species. Nat. Biotechnol. 36, 411–420.

Chao, C.C., Hu, S., Sheng, W.S., and Peterson, P.K. (1995). Tumor necrosis factor-alpha production by human fetal microglial cells: regulation by other cytokines. Dev. Neurosci. 17, 97–105.

Collado, M.C., Rautava, S., Aakko, J., Isolauri, E., and Salminen, S. (2016). Human gut colonisation may be initiated in utero by distinct microbial communities in the placenta and amniotic fluid. Sci. Rep. 6, 23129.

Durek, P., Nordstro¨ m, K., Gasparoni, G., Salhab, A., Kressler, C., de Almeida, M., Bassler, K., Ulas, T., Schmidt, F., Xiong, J., et al.; DEEP Consortium (2016). Epigenomic profiling of human CD4+ T cells supports a linear differentiation model and highlights molecular regulators of memory development. Immunity 45, 1148–1161.

Eilers, M., Schirm, S., and Bishop, J.M. (1991). The MYC protein activates transcription of the alpha-prothymosin gene. EMBO J. 10, 133–141.

Fan, Z., Beresford, P.J., Oh, D.Y., Zhang, D., and Lieberman, J. (2003). Tumor suppressor NM23-H1 is a granzyme A-activated DNase during CTL-mediated apoptosis, and the nucleosome assembly protein SET is its inhibitor. Cell 112, 659–672.

Gerner, R.R., Klepsch, V., Macheiner, S., Arnhard, K., Adolph, T.E., Grander, C., Wieser, V., Pfister, A., Moser, P., Hermann-Kleiter, N., et al. (2018). NAD metabolism fuels human and mouse intestinal inflammation. Gut 67, 1813–1823.

Gibbons, D., Fleming, P., Virasami, A., Michel, M.-L., Sebire, N.J., Costeloe, K., Carr, R., Klein, N., and Hayday, A. (2014). Interleukin-8 (CXCL8) production is a signatory T cell effector function of human newborn infants. Nat. Med. 20, 1206–1210.

Granot, T., Senda, T., Carpenter, D.J., Matsuoka, N., Weiner, J., Gordon, C.L., Miron, M., Kumar, B.V., Griesemer, A., Ho, S.H., et al. (2017). Dendritic cells display subset and tissue-specific maturation dynamics over human life. Immunity 46, 504–515.

Grün, D., and van Oudenaarden, A. (2015). Design and analysis of single-cell sequencing experiments. Cell 163, 799–810.

Hashimshony, T., Senderovich, N., Avital, G., Klochendler, A., de Leeuw, Y., Anavy, L., Gennert, D., Li, S., Livak, K.J., Rozenblatt-Rosen, O., et al. (2016). CEL-Seq2: sensitive highly-multiplexed single-cell RNA-Seq. Genome Biol. 17, 77.

Haynes, B.F., and Heinly, C.S. (1995). Early human T cell development: analysis of the human thymus at the time of initial entry of hematopoietic stem cells into the fetal thymic microenvironment. J. Exp. Med. 181, 1445–1458.

He, Y.-M., Li, X., Perego, M., Nefedova, Y., Kossenkov, A.V., Jensen, E.A., Kagan, V., Liu, Y.-F., Fu, S.-Y., Ye, Q.-J., et al. (2018). Transitory presence of myeloid-derived suppressor cells in neonates is critical for control of inflammation. Nat. Med. 24, 224–231.

Hilliard, B.A., Mason, N., Xu, L., Sun, J., Lamhamedi-Cherradi, S.E., Liou, H.C., Hunter, C., and Chen, Y.H. (2002). Critical roles of c-Rel in autoimmune inflammation and helper T cell differentiation. J. Clin. Invest. 110, 843–850.

Karin, M., and Clevers, H. (2016). Reparative inflammation takes charge of tissue regeneration. Nature 529, 307–315.

Kivioja, T., Vähärautio, A., Karlsson, K., Bonke, M., Enge, M., Linnarsson, S., and Taipale, J. (2011). Counting absolute numbers of molecules using unique molecular identifiers. Nat. Methods 9, 72–74.

Klarenbeek, P.L., Tak, P.P., van Schaik, B.D.C., Zwinderman, A.H., Jakobs, M.E., Zhang, Z., van Kampen, A.H.C., van Lier, R.A.W., Baas, F., and de Vries, N. (2010). Human T-cell memory consists mainly of unexpanded clones. Immunol. Lett. 133, 42–48.

Kotlyarov, A., Neininger, A., Schubert, C., Eckert, R., Birchmeier, C., Volk, H.D., and Gaestel, M. 94–97.

Kretzschmar, K., and Clevers, H. (2017). Wnt/β-catenin signaling in adult mammalian epithelial stem cells. Dev. Biol. 428, 273–282.

Kuprash, D.V., Tumanov, A.V., Liepinsh, D.J., Koroleva, E.P., Drutskaya, M.S., Kruglov, A.A., Shakhov, A.N., Southon, E., Murphy, W.J., Tessarollo, L., et al. (2005). Novel tumor necrosis factor-knockout mice that lack Peyer's patches. Eur. J. Immunol. 35, 1592–1600.

Le Saout, C., Mennechet, S., Taylor, N., and Hernandez, J. (2008). Memory like CD8+ and CD4+ T cells cooperate to break peripheral tolerance under lymphopenic conditions. Proc. Natl. Acad. Sci. USA 105, 19414–19419.

Lehtinen, M.K., Yuan, Z., Boag, P.R., Yang, Y., Ville´ n, J., Becker, E.B.E., DiBacco, S., de la Iglesia, N., Gygi, S., Blackwell, T.K., and Bonni, A. (2006). A conserved MST-FOXO signaling pathway mediates oxidative-stress responses and extends life span. Cell 125, 987–1001.

Lindemans, C.A., Calafiore, M., Mertelsmann, A.M., O'Connor, M.H., Dudakov, J.A., Jenq, R.R., Velardi, E., Young, L.F., Smith, O.M., Lawrence, G., et al. (2015). Interleukin-22 promotes intestinal-stem-cell-mediated epithelial regeneration. Nature 528, 560–564.

Love, M.I., Huber, W., and Anders, S. (2014). Moderated estimation of fold change and dispersion for RNA-seq data with DESeq2. Genome Biol. 15, 550.

Mackay, L.K., Stock, A.T., Ma, J.Z., Jones, C.M., Kent, S.J., Mueller, S.N., Heath, W.R., Carbone, F.R., and Gebhardt, T. (2012). Long-lived epithelial immunity by tissue-resident memory T (TRM) cells in the absence of persisting local antigen presentation. Proc. Natl. Acad. Sci. USA 109, 7037–7042.

Maloy, K.J., and Powrie, F. (2011). Intestinal homeostasis and its breakdown in inflammatory bowel disease. Nature 474, 298–306.

Masopust, D., Choo, D., Vezys, V., Wherry, E.J., Duraiswamy, J., Akondy, R., Wang, J., Casey, K.A., Barber, D.L., Kawamura, K.S., et al. (2010). Dynamic T cell migration program provides resident memory within intestinal epithelium. J. Exp. Med. 207, 553–564.

McGovern, N., Shin, A., Low, G., Low, D., Duan, K., Yao, L.J., Msallam, R., Low, I., Shadan, N.B., Sumatoh, H.R., et al. (2017). Human fetal dendritic cells promote prenatal T-cell immune suppression through arginase-2. Nature 546, 662–666.

Meienhofer, M.C., Lagrange, J.L., Cottreau, D., Lenoir, G., Dreyfus, J.C., and Kahn, A. (1979). Phosphofructokinase in human blood cells. Blood 54, 389–400.

Mendillo, M.L., Santagata, S., Koeva, M., Bell, G.W., Hu, R., Tamimi, R.M., Fraenkel, E., Ince, T.A., Whitesell, L., and Lindquist, S. (2012). HSF1 drives a transcriptional program distinct from heat shock to support highly malignant human cancers. Cell 150, 549–562.

Micha€elsson, J., Mold, J.E., McCune, J.M., and Nixon, D.F. (2006). Regulation of T cell responses in the developing human fetus. J. Immunol. 176, 5741–5748.

Mold, J.E., Michaëlsson, J., Burt, T.D., Muench, M.O., Beckerman, K.P., Busch, M.P., Lee, T.-H., Nixon, D.F., and McCune, J.M. (2008). Maternal alloantigens promote the development of tolerogenic fetal regulatory T cells in utero. Science 322, 1562–1565.

Mor, G., Aldo, P., and Alvero, A.B. (2017). The unique immunological and microbial aspects of pregnancy. Nat. Rev. Immunol. 17, 469–482.

Mueller, S.N., and Mackay, L.K. (2016). Tissue-resident memory T cells: local specialists in immune defence. Nat. Rev. Immunol. 16, 79–89.

Neu, J., and Walker, W.A. (2011). Necrotizing enterocolitis. N. Engl. J. Med. 364, 255–264.

Nusse, Y.M., Savage, A.K., Marangoni, P., Rosendahl-Huber, A.K.M., Landman, T.A., de Sauvage, F.J., Locksley, R.M., and Klein, O.D. (2018). Parasitic helminths induce fetal-like reversion in the intestinal stem cell niche. Nature 559, 109–113.

Orosz, P., Echtenacher, B., Falk, W., Rüschoff, J., Weber, D., and Männel, D.N. (1993). Enhancement of experimental metastasis by tumor necrosis factor. J. Exp. Med. 177, 1391–1398.

Parekh,S., Ziegenhain,C., Vieth, B.,Enard,W., andHellmann, I. (2018). zUMIs – A fast and flexible pipeline to process RNA sequencing data with UMIs. Gigascience 7, 1–9.

Powrie, F., Leach, M.W., Mauze, S., Menon, S., Caddle, L.B., and Coffman, R.L. (1994). Inhibition of Th1 responses prevents inflammatory bowel disease in scid mice reconstituted with CD45RBhi CD4+ T cells. Immunity 1, 553–562.

Prendergast, A.J., Klenerman, P., and Goulder, P.J.R. (2012). The impact of differential antiviral immunity in children and adults. Nat. Rev. Immunol. 12, 636–648.

Rautava, S., Luoto, R., Salminen, S., and Isolauri, E. (2012). Microbial contact during pregnancy, intestinal colonization and human disease. Nat. Rev. Gastroenterol. Hepatol. 9, 565–576.

Sands, B.E., and Kaplan, G.G. (2007). The role of TNFα in ulcerative colitis. J. Clin. Pharmacol. 47, 930–941.

Sato, T., and Clevers, H. (2013). Growing self-organizing mini-guts from a single intestinal stem cell: mechanism and applications. Science 340, 1190–1194.

Schoenberger, S.P. (2012). CD69 guides CD4+ T cells to the seat of memory. Proc. Natl. Acad. Sci. USA 109, 8358–8359.

Schreurs, R.R.C.E., Drewniak, A., Bakx, R., Corpeleijn, W.E., Geijtenbeek, T.B.H., van Goudoever, J.B., and Bunders, M.J. (2017). Quantitative comparison of human intestinal mononuclear leukocyte isolation techniques for flow cytometric analyses. J. Immunol. Methods 445, 45–52.

Schwitalla, S., Fingerle, A.A., Cammareri, P., Nebelsiek, T., Göktuna, S.I., Ziegler, P.K., Canli, O., Heijmans, J., Huels, D.J., Moreaux, G., et al. (2013). Intestinal tumorigenesis initiated by dedifferentiation and acquisition of stem-cell-like properties. Cell 152, 25–38.

Sharpe, A.H., Wherry, E.J., Ahmed, R., and Freeman, G.J. (2007). The function of programmed cell death 1 and its ligands in regulating autoimmunity and infection. Nat. Immunol. 8, 239–245.

Stefanini, M. (1972). Chronic hemolytic anemia associated with erythrocyte enolase deficiency exacerbated by ingestion of nitrofurantoin. Am. J. Clin. Pathol. 58, 408–414.

Tang, F., Barbacioru, C., Wang, Y., Nordman, E., Lee, C., Xu, N., Wang, X., Bodeau, J., Tuch, B.B., Siddiqui, A., et al. (2009). mRNA-seq whole-transcriptome analysis of a single cell. Nat. Methods 6, 377–382.

Thome, J.J.C., Bickham, K.L., Ohmura, Y., Kubota, M., Matsuoka, N., Gordon, C., Granot, T., Griesemer, A., Lerner, H., Kato, T., and Farber, D.L. (2016). Early-life compartmentalization of human T cell differentiation and regulatory function in mucosal and lymphoid tissues. Nat. Med. 22, 72–77.

van der Flier, L.G., van Gijn, M.E., Hatzis, P., Kujala, P., Haegebarth, A., Stange, D.E., Begthel, H., van den Born, M., Guryev, V., Oving, I., et al. (2009). Transcription factor achaete scute-like 2 controls intestinal stem cell fate. Cell 136, 903–912.

van Dongen, J.J.M., Langerak, A.W., Brüggemann, M., Evans, P.A.S., Hummel, M., Lavender, F.L., Delabesse, E., Davi, F., Schuuring, E., Garcı´a-Sanz, R., et al. (2003). Design and standardization of PCR primers and protocols for detection of clonal immunoglobulin and T-cell receptor gene recombinations in suspect lymphoproliferations: report of the BIOMED-2 concerted action BMH4-CT98-3936. Leukemia 17, 2257–2317.

Weaver, L.T., Austin, S., and Cole, T.J. (1991). Small intestinal length: a factor essential for gut adaptation. Gut 32, 1321–1323. Weitkamp, J.-H., Koyama, T., Rock, M.T., Correa, H., Goettel, J.A., Matta, P., Oswald-Richter, K., Rosen, M.J., Engelhardt, B.G., Moore, D.J., and Polk, D.B.

(2013). Necrotising enterocolitis is characterised by disrupted immune regulation and diminished mucosal regulatory (FOXP3)/effector (CD4, CD8) T cell ratios. Gut 62, 73–82.

Yu, G., Wang, L.-G., Han, Y., and He, Q.-Y. (2012). clusterProfiler: an R package for comparing biological themes among gene clusters. OMICS 16, 284–287.

Zhang, X., Mozeleski, B., Lemoine, S., Dériaud, E., Lim, A., Zhivaki, D., Azria, E., Le Ray, C., Roguet, G., Launay, O., et al. (2014). CD4 T cells with effector memory phenotype and function develop in the sterile environment of the fetus. Sci. Transl. Med. 6, 238ra72.

Zolti, M., Ben-Rafael, Z., Meirom, R., Shemesh, M., Bider, D., Mashiach, S., and Apte, R.N. (1991). Cytokine involvement in oocytes and early embryos. Fertil. Steril. 56, 265–272.

STAR METHODS

Experimental model and subject details

Samples

Fetal intestinal and mesenteric lymph node tissues were obtained from 50 fetal donors (median gestational age 17 weeks, IQR 16-18 weeks) by the HIS Mouse Facility of the Amsterdam University Medical Center (AUMC), Amsterdam. All fetal material was collected from donors from whom a written informed consent for the use of the material for research purposes was obtained by the Bloemenhove clinic (Heemstede, the Netherlands). These informed consents are kept together with the medical record of the donor by the clinic. Not all samples were used for all assays due to the limited numbers of cells isolated from the tissues. Infant tissues (ileum or colon) and one cord blood sample from 27 healthy (non-inflamed) infant donors (median age 4 months, IQR 2-8 months) were obtained. Infant tissues were obtained at intestinal surgery due to congenital abnormalities at the Pediatric Surgery Center of Amsterdam (AUMC) and the University Medical Center Hamburg-Eppendorf. Tissues from 14 infants diagnosed with NEC (median gestational age of 25.5 weeks, IQR 24-28 weeks) were obtained at surgery to resect inflamed intestinal tissue at the Pediatric Surgery Center of Amsterdam (AUMC) and the University Medical Center Hamburg-Eppendorf. Tissues from 3 prematurely born infants without NEC (gestational ages two infant born at 25 weeks gestation and one infant born at 26 weeks gestation) were collected at surgery at the Pediatric Surgery Center of Amsterdam (AUMC) and the University Medical Center Hamburg-Eppendorf. Blood and cord blood samples were obtained anonymously from healthy volunteers at the AUMC, Amsterdam. Donor specifics are provided in **Table S1**. Donors or the guardians of pediatric donors provided informed consent for the use of materials in this study. Tissues were obtained in Amsterdam with approval of the ethical committee of the AUMC (University of Amsterdam) and in Hamburg with approval of the ethics committee of the medical association of the Freie Hansestadt Hamburg (Ärztekammer Hamburg) and in accordance with the Declaration of Helsinki. The intestinal tissue of an adult pregnant C57BL/6J mouse and 3 pups of her litter were obtained in accordance with the Institutional Review Board "Behörde für Soziales, Familie, Gesundheit und Verbraucherschutz" (Hamburg, Germany).

Method details

Lymphocyte isolation from human blood and tissue specimens

Blood and tissue samples were processed in the laboratory within 12 hours of procurement. Blood samples were collected in heparine-coated tubes. The mononuclear cell fraction was isolated using a density gradient. Blood was diluted 1:1 with Hank's Balanced Salt Solution (HBSS; Lonza), then layered on top of Lymphoprep (Axis-Shield) and centrifuged for 22 minutes at room temperature at 1000G with 120 seconds acceleration and no break. The mononuclear cell fraction was aspirated and washed with phosphate buffered saline (PBS). Mesenteric lymph nodes were cleaned with PBS after which the tissue was minced with scissors and digested for 2x 30 minutes at 37°C with Iscove's Modified Dulbecco's Medium (IMDM; Lonza)

supplemented with 1 mg/ml (0.15 U/mg) Collagenase D (Roche), 1% fetal bovine serum (FBS; Biological Industries), and 1000 U/ml DNAse type I (Worthington Biochemical Corporation). The supernatant containing the cells was filtered through a 70 µm strainer (Falcon, Corning) to obtain a single cell solution. Lymphocytes were then isolated by density gradient centrifugation using Lymphoprep as described for blood samples. Intestinal lymphocytes were isolated as described before (Schreurs et al., 2017). Fetal intestines were cut open longitudinally and cleaned from meconium by washing in PBS until PBS was clear. Intestinal tissues from older donors were washed with PBS until PBS was clear after which the muscle layer was removed with scissors and again washed if needed. Sizes of the intestinal tissues without the muscle layer were documented. Intestinal tissues were next cut into 0.5x0.5 cm segments and incubated for 2x 20 minutes, in a shaking water bath (100 strokes/minute), at 37°C with IMDM supplemented with 5 mM ethylenediaminetetraacetic acid (EDTA; Sigma-Aldrich), 2 mM 1,4-dithiothreitol (DTT; Sigma-Aldrich) and 1% FBS to detach the epithelial layer. The supernatant was filtered through a 70 µm cell strainer to obtain a single cell solution. Epithelial lymphocytes were isolated by density gradient centrifugation using Lymphoprep as described for blood lymphocytes. The intestinal tissue, now devoid of the epithelial layer, was minced and digested for 2x 30 minutes at 37°C with IMDM (Lonza) supplemented with 1 mg/ml (0.15 U/mg) Collagenase D (Roche), 1% fetal bovine serum (FBS; Biological Industries), and 1000 U/ml DNAse type I (Worthington Biochemical Corporation). The supernatant containing the cells was filtered through a 70 µm strainer (Falcon, Corning) to obtain a single cell solution. Lamina propria lymphocytes were isolated from the single cell suspension using a Percoll gradient (Sigma-Aldrich); standard isotonic Percoll solution (SIP) was prepared by supplementing 100% Percoll with 10% 10X PBS, using an additional 1X PBS resulted in 60% SIP solution. After isolation, the number of viable cells was counted using Trypan blue (Sigma-Aldrich).

Lymphocyte isolation from murine tissue specimens

One adult (10-14 week old) pregnant C57BL/6J mouse and her pups were sacrificed in the late stage of pregnancy (day 19.5), and the fetuses were excised. The intestines were harvested. Peyer's patches from maternal intestines were excised. Maternal and fetal small and large intestine was separated, cut longitudinally and washed with PBS until clear. For isolation of intraepithelial lymphocytes, the intestinal tissue was incubated in HBSS (Gibco) supplemented with 17% 10X HEPES (Sigma-Aldrich), 17% FBS (Gibco), and 1 mM DTT (Sigma-Aldrich) for 20 minutes at 37°C, shaking (200 strokes/min). The remaining tissue was then minced and incubated from 40 minutes at 37°C, shaking (200 strokes/min) in Roswell Park Memorial Institute (RPMI; Sigma-Aldrich) 1640 medium, supplemented with 1 mM $CaCl_2$ (Sigma-Aldrich), 1 mM $MgCl_2$ (Sigma-Aldrich), 1% FBS, 1 mg/ml Collagenase NB 6 (Serva), and 10 U/ml DNAse I (Roche) to collect lamina propria lymphocytes. Epithelial and lamina propria-derived lymphocytes were further enriched by Percoll gradient centrifugation (GE Healthcare).

Stimulation assays for cytokine production by lymphocytes

Cells were resuspended in IMDM supplemented with 10% FBS (Biological Industries), 50 µg/ml Gentamicin (Gibco) and 60 µM 2-mercaptoethanol (Sigma-Aldrich) and either left unstimulated, stimulated with 1.5 µg/ml anti-CD3 (1XE; Sanquin) and 2 µg/ml anti-CD28 (15E8; Sanquin), or stimulated with 10 ng/ml phorbol 12-myristate 13-acetate (PMA; Sigma-Aldrich) and 1 µg/ml ionomycin (Sigma-Aldrich), a relatively low concentration, for 12 hours. 7 µg/ml brefeldin A (Sigma-Aldrich) was added after one hour incubation. Cells were kept at 37°C and 5% CO_2 for the duration of the stimulation. In flow cytometric analyses of cytokine production, unstimulated cells are represented by viable $CD45^+CD3^+CD4^+$ cells, stimulations with anti-CD3 and anti-CD28 (TCR) by viable $CD45^+CD4^+CD8^-$ cells, and stimulations with PMA-ionomycin (P/I) by viable $CD45^+CD3^+CD8^-$ cells. These populations were chosen as TCR-stimulations do not allow for CD3 detection and P/I-stimulations can downregulate CD4 to some degree. The contribution of non-$CD4^+$ T cells to the $CD3^+8^-$ population was minimal in the lamina propria tissues (**Figure S1C and Figure S6B**). Studies were performed using lamina propria-derived $CD4^+$ T cells due to the limited cell numbers isolated from intestinal epithelium.

Flow cytometry

For surface molecule staining, cells were incubated with antibodies (see Key Resources table for all antibodies) in PBS for 30 minutes at 4°C on a shaker (600 strokes/minute), washed and fixated with 1X stabilizing fixative (BD Bioscience). For intracellular molecule staining (see Key Resources table for all antibodies), surface-stained cells were washed, fixated with 1X Fixation/Permeabilization reagent (eBioscience) for 15 minutes on a shaker (600 strokes/minute) and incubated with antibodies in 1X Permeabilization Buffer (eBioscience) for 30 minutes at 4°C on a shaker (600 strokes/minute). Ultracomp eBeads (eBioscience) were used to determine spectral overlap. Stained cells were acquired on a LSR Fortessa Flow Cytometer (BD Biosciences) using FACSDIVA software (version 8; BD Biosciences) within 24 hours after staining and analyzed using FlowJo software (version 10.5.0; Treestar). Murine stained cells were acquired on a LSRII Flow Cytometer (BD). For t-distributed stochastic neighbor embedding (t-SNE) analyses within FlowJo software (Version 10.5.0), the $CD4^+$ T cell population was first downsampled to 10,000 events. Relevant compensated parameters were selected and subsequently two new parameters (t-SNE1 and t-SNE2) were created, allowing for the visualization of the size and overlap of multiple fluorescent labels of interest in one t-SNE plot.

TCR RNA Sequencing

Fetal and infant epithelial and lamina proria-derived sorted $CD4^+$ Tem cells were collected and lysed in 350 µL Buffer RLT (Qiagen) plus 1% 2-mercaptoethanol (Sigma-Aldrich) and stored at -80°C until RNA isolation, performed with RNeasy Mini Kit (Qiagen) according to the manufacturer's instructions. cDNA was synthesized with custom primers containing: a specific sequence for TCRβ C region (Klarenbeek et al., 2010), a Unique Molecular Identifier (UMIs) (Kivioja et al., 2012) and MiSeq (Illumina) sequencing adaptors. cDNA synthesis was

performed using SuperScript™ III Reverse Transcriptase (Thermo Fisher Scientific) according to manufacturer's instructions for custom primers. cDNA was purified using Agencourt AMPure XP beads (Beckman Coulter) using 1:1 ratio. Purified cDNA (125 ng) was used for PCR using TCRβ V genes forward primers (adapted from van Dongen et al., 2003) and MiSeq adaptor sequences as reverse primers. PCR was performed using HOT FIREPol® DNA Polymerase (Solis BioDyne) as follows: 96°C 15 minutes, 40× (96°C for 30 seconds, 60°C for 60 seconds, 72°C for 30 seconds), 72°C for 10 minutes. The PCR products were purified (Agencourt AMPure XP beads) and further processed for Next-Generation Sequencing (NGS). Purified PCR products were processed for NGS using MiSeq Reagent Kit v3 600 cycles (Illumina) according to the manufacturer's instructions. Sequencing was performed on the Illumina MiSeq platform. 3102 clones per sample were randomly selected and used for analysis. TCRβ clones were identified according to their unique V-CDR3-J combination via a customized bioinformatics pipeline as described earlier (Klarenbeek et al., 2010).

CD4⁺ T cell sorting and subsequent single-cell RNA-sequencing

Unstimulated intestinal epithelial and lamina propria mononuclear cells were surface stained as described and $CD4^+$ Tem cells (viable $CD45^+3^+4^+CCR7^-CD45RA^-CD45R0^+$) and non-effector cells (viable $CD45^+3^+4^+CCR7^+$) were single-cell sorted, using a 4-laser FACS Aria IIu SORP (BD Biosciences) and FACSDIVA software (BD Biosciences), directly into a 384-well plate provided by the single cell sequencing facility (Hubrecht Institute, Utrecht, the Netherlands). $CD4^+$ Tn and $CD4^+$ Tcm were combined due to very low numbers of these cells in fetal intestines ($CD45^+3^+4^+CCR7^+$). Furthermore, $CD4^+$ Tem cells were sorted in a tube and stimulated for 6 hours with PMA-ionomycin and subsequently sorted into a 384-well plate. Cells were directly dissolved in primer mix. Single cell library preparation and sequencing single cell RNA-seq Libraries were prepared using the CEL-Seq2 protocol as previously described (Hashimshony et al., 2016). cDNA libraries were sequenced on an Illumina NextSeq500 using 75bp paired-end sequencing (Utrecht Sequencing Facility).

Single CD4⁺ T cell RNA-sequencing data analysis

Reads obtained from sequencing fetal and infant T cells were mapped and deconvoluted into single cell transcriptomes using the zUMIs pipeline (version 2.0.5) (Parekh et al., 2018). This included mapping with STAR 2.6.0c and counting with Rsubread 1.30.5. GRCh38 was used as a reference genome. All further analysis steps were performed in R 3.5.1 using the Seurat framework (version 2.3.4) (Butler et al., 2018). First, all cells were combined into one Seurat single cell object. Cells with less than 100 detected genes were removed as well as genes expressed in less than 50 cells and cells with more than 25% of reads from mitochondrially encoded genes. Expression data was normalized and scaled with regression on number of detected genes (nGene) and number of detected unique molecular identifiers (nUMI). Outliers in a nGene/nUMI plot were removed from the dataset. One small cluster of cells was positive for myeloid cell markers and was removed from the dataset. In total 2147 fetal intestinal T cells and 754

infant intestinal T cells were part of the final dataset, with an overall smaller gene detection rate for the infant cells. For data visualization, t-SNE plots of all unstimulated or all stimulated (PMA and ionomycin) cells were generated based on a principal component analysis (PCA) of the most variable genes in the dataset. Gene ontology (GO) term enrichment analysis was performed on a pseudo bulk of all CD4+ Tem cells in each group to take into account potential quality differences. Specifically, genes were sorted by their summarized expression values and subjected to the gseGO() function of the clusterProfiler package (Yu et al., 2012) using standard settings and an adjusted p-value cutoff of 0.05 to determine GO biological process terms characterizing the transcriptomic signatures of both groups. A network of GO terms uniquely found in fetal intestinal CD4+ Tem cells was calculated using the emapplot() function to visualize genes shared between terms. The resulting plot was modified for clarity by curating groups of similar GO terms and assigning representative labels. Analysis of the enrichment of representative GO terms on a single cell level was performed using the AUCell algorithm (Aibar et al., 2017) and resulting area under the curve (AUC) values were plotted for each cell individually. To identify a stimulation specific signature for fetal intestinal CD4+ Tem cells, differentially expressed genes were determined for pseudo-bulks of all stimulated versus all unstimulated fetal CD4+ Tem cells using DESeq2 (Love et al., 2014) with inclusion of donor identity in the modelling and an adjusted p-value cutoff of 0.05. To identify differences compared to infant intestinal CD4+ Tem cells the results were filtered for genes with detection in at least 20 stimulated infant CD4+ Tem cells and the Seurat inherent function FindMarkers() was used to determine which candidate genes were differentially expressed between fetal and infant intestinal CD4+ Tem cells (adjusted p-value cutoff 0.05). Selected genes were visualized in a heatmap.

Intestinal organoid culture

The epithelial layer from fetal intestines, containing the intestinal stem cells (ISCs), was detached using EDTA and DTT as described in the segment "Lymphocyte isolation from human blood and tissue specimens", with the modification that tissues were incubated at 4°C for 1 hour on a shaker (600 strokes/minute). Single cells were suspended in 10 µl Matrigel (Corning) drops, with 3 drops per well of a 24-well plate. The Matrigel was allowed to solidify for 10 minutes at 37°C after which 0.5 ml human intestinal stem cell medium (HISC) was added to each well. HISC comprises Advanced Dulbecco Modified Eagle Medium (DMEM)/F12 supplemented with 1% 1X GlutaMAX, 1% 1X Penicillin/Streptomycin, 1:25 1X B27 supplement, 1:50 1X N2 supplement, 1:500 1X mouse epidermal growth factor (EGF; all Invitrogen), 1% 1M HEPES, 500 mM n-Acetyl-L-cysteine, 10 µM [Leu^{15}]-Gastrin, 1M Nicotinamid, 20 mM SB202190 (all Sigma-Aldrich), Noggin 20%, Rspondin 10%, WNT3a (all three AUMC conditioned home-made medium), 500 µM A83-01 (Tocris), and 10 µM ROCK inhibitor (Stemcell Technologies). Medium was refreshed every 2-3 days. Once the organoids developed (5-10 days after initial seeding), they were passaged once per week to remove dead cells, debris, and to break up larger organoids. To passage organoids, the organoids were taken up in ice-cold advanced DMEM/F12 supplemented with 1% 1X GlutaMAX, 1% 1X Penicillin/Streptomycin, and 1% 1M HEPES.

The organoids were broken up with two repeating pipetting cycles (20x vigorous pipetting) using tips of 200 µl and 20 µl volume. If needed single cell suspension was obtained upon treatment of the organoids with TrypLE express (Invitrogen) for 5-7 minutes at 37°C. Upon a minimum of three passages organoids were used for experiments. Organoid development was monitored for 12 days in HISC medium supplemented with 0, 0.2, 2, 20, 200 ng/ml recombinant human (rh) TNF-α (Bio-Techne). Medium (including rh-TNF-α) was refreshed every 2-3 days. Organoid development was measured by taking 5X and 20X images with a Leica (DM IRB) inverted microscope on day 12. The images were used to count the number of organoids using ImageJ (version 1.50i) software. Organoids were collected for subsequent RNA-seq.

Furthermore, we developed $CD4^+$ T cell-ISC co-culture systems. Fetal lamina propria mononuclear cells were surface stained as described and $CD4^+$ Tem cells (viable $CD45^+CD3^+CD4^+CCR7^-CD45RA^-$) were sorted, using a 4-laser FACS Aria IIu SORP (BD Biosciences) and FACSDIVA software (BD Biosciences). Cells were resuspended in IMDM supplemented with 10% FBS (Biological Industries), 50 µg/ml Gentamicin (Gibco) and 60 µM 2-mercaptoethanol (Sigma-Aldrich) and stimulated with 1.5 µg/ml anti-CD3 (1XE; Sanquin) and 2 µg/ml anti-CD28 (15E8; Sanquin) for 2 hours. Cells were kept at 37°C and 5% CO_2 for the duration of the stimulation. T cells were seeded together with ISCs in 10 µl drops of Matrigel at the desired concentration of T cells per µl Matrigel. Organoid development was monitored for up to 10 days in HISC medium without SB202190 (Sigma-Aldrich) and supplemented with 50 U/ml IL-2 (Miltenyi) and 0.38 µg/ml TNF-α-block (human TNF RI/TNFRSF1A MAb; Bio-techne) where appropriate. Medium (including supplements) was refreshed every 2-3 days. Organoid development was measured by taking images with a Leica (DM IRB) inverted microscope. The images (one image represents one field of view; FOV) were used to count the number of the organoids using ImageJ (version 1.50i) software.

RNA isolation and RT-qPCR

RNA was isolated from *ex vivo* surgically removed intestinal tissues, using TRIzol (Thermo Fisher Scientific) according to the manufacturer's instructions. Briefly, samples were lysed in TRIzol, RNA was separated with chloroform (Merck), precipitated with 2-isopropanol (Merck) and washed with 75% ethanol in nucleotide-free H_2O. To evaluate *TNFA, NFKBIA, TNFAIP2, and TNFAIP3* expression, cDNA was prepared using a reverse transcription kit (Promega) as per the manufacturer's instructions. cDNA templates were mixed with primers and SYBR Green (Applied Biosystems) and the RT-qPCR reaction was performed on a 7500 Fast System (Applied Biosystems). Ct-values normalized to *GAPDH* were used to generate gene expression values. To evaluate *LGR5* expression in ISCs from organoids, RNA was isolated as described and cDNA was synthesized using the iScript cDNA synthesis kit (BioRad) and used in a subsequent RT-qPCR with the SYBR Green supermix (BioRad) in a T100 Thermal Cycler (BioRad) according to the manufacturer's protocol. Acquired mean Ct-values from technical duplicates were analyzed using the comparative ΔCt method and normalized to *ACTB*.

Whole genome RNA-sequencing of organoids

For whole genome RNA sequencing of ISC from organoid cultures, RNA was isolated as described. The polyadenylated mRNA fraction was isolated using NEXTflex Poly(A) Beads (Bioo Scientific) and sequencing libraries were constructed using the NEXTflexRapid Directional RNA-seq kit (Bioo Scientific). Libraries were sequenced on the Nextseq500 platform (Illumina), producing single-end reads of 75 bp. Reads were aligned to the human reference genome GRCh37 using STAR (version 2.4.2a). Picard's AddOrReplaceReadGroups (v1.98) was used to add read groups to the BAM files, which were sorted with Sambamba (version 0.4.5) and transcript abundances were quantified with HTSeq-count (version 0.6.1p1) using union mode. Subsequently, reads per kilobase million reads sequenced (RPKMs) were calculated with edgeR's RPKM function.

Immunohistochemistry (IHC)

Sections of formalin-fixed paraffin-embedded human intestinal tissue samples were dewaxed and rehydrated, after which they were stained in an automatic immunostainer (Benchmark Ultra; Ventana Medical Systems). Tissue specimens were stained for structural components with hematoxylin & eosin (Klinipath & Merck) and T cells cells were visualized with an antibody against CD3 (Thermo Fisher Scientific), using a 3,3'-diaminobenzidine detection kit (OptiViewDAB; Ventana medical Systems) and counterstaining cell nuclei with hematoxylin II and bluing agent (both Ventana Medical Systems). Stained tissue samples were evaluated and images were acquired (10X) using a Leica (DM IRB) inverted microscope.

Statistical analysis

Statistical significance of differences was assessed using nonparametric Mann-Whitney U tests, or ANOVAs where appropriate. The software package Graphpad Prism (version 7; GraphPad Software) was used to analyze data and to perform statistical analyses. Median frequencies and interquartile ranges (IQRs) are given in figures and text unless otherwise stated. Values of $p < 0.05$ were considered significant. Details on statistical tests used, the value of n and what the data represent can be found in the respective figure legends.

SUPPLEMENTAL INFORMATION

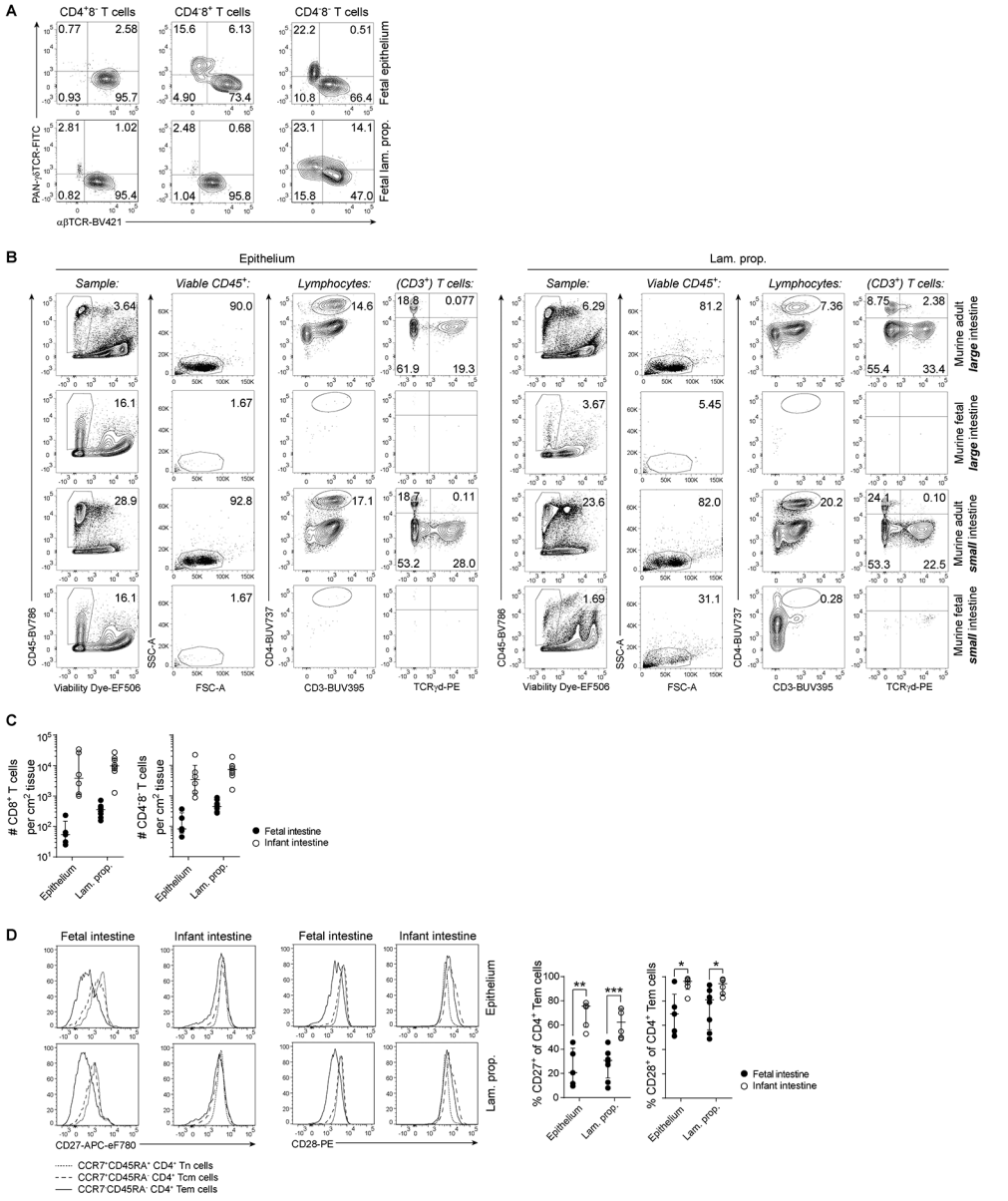

Figure S1. CD4⁺ T effector memory cells are present in human but not murine fetal intestines (see also Figure 1). (A) Representative flow cytometric plots showing the expression of αbTCR and γdTCR on epithelial and lamina propria (lam. prop)-derived $CD4^+8^-$, $CD4^-8^+$, and $CD4^-8^-$ T cells. (B) Representative flow cytometric plots of mononuclear cells isolated from murine adult and fetal intestines and showing expression of CD3, CD4, and γdTCR. Studies were performed in murine adult (n=1) and murine fetal large and small intestines (n=3). (C) Median count (± IQR) of fetal and infant epithelium and lam. prop.-derived $CD8^+$ and $CD4^-8^-$ T cells per cm^2 tissue. Fetal epithelium (n=5) and lam. prop. intestinal tissues (n=8), infant ▸

epithelium (n=6) and lam. prop. intestinal tissues (n=8). (D) Overlays of median fluorescence intensity of CD27 and CD28 on epithelial and lam. prop. CD4+ Tn (CCR7+CD45RA+), Tcm (CCR7+CD45RA-), and Tem (CCR7-CD45RA-) cells from fetal and infant intestines and median percentage (± IQR) CD27+CD4+ Tem cells and CD28+CD4+ Tem cells. Tn = naïve T cell, Tcm = central memory T cell, Tem = effector memory T cell. Fetal epithelium (n=5) and lam. prop. intestinal tissues (n=8), infant epithelium (n=6) and lam. prop. intestinal tissues (n=6). Mann-Whitney U comparisons. *p<0.05, ** p<0.01, ***p<0.001.

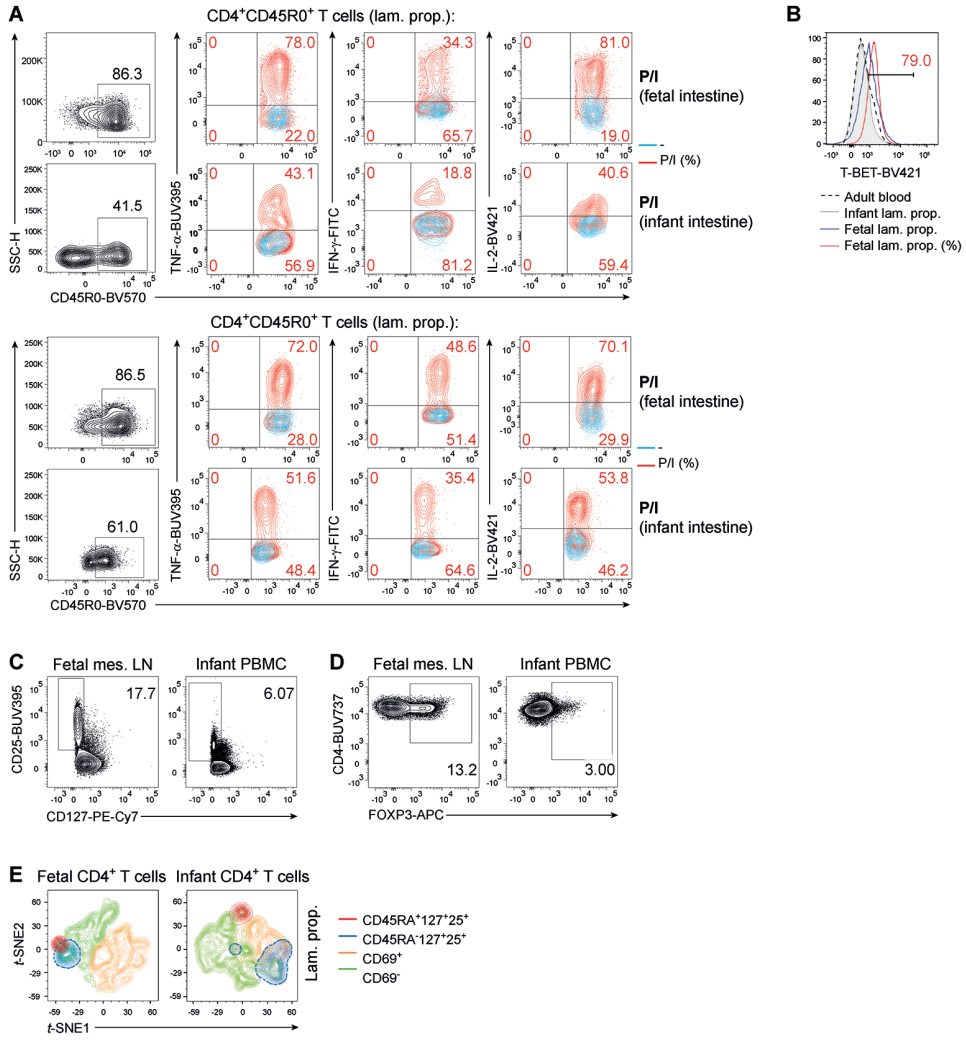

Figure S2. Fetal intestinal CD4+ T cells produce Th1-related cytokines (see also Figure 3). (A) Flow cytometric plots of TNF-α, IFN-γ and IL-2 expression in PMA and ionomycin (P/I)-stimulated CD45R0+CD4+ T cells in fetal and infant intestinal lamina propria (lam. prop.) tissues in two fetal and two infant donors. P/I-stimulated CD4+ T cells are shown in red (including percentages), while unstimulated (-) CD4+ T cells used as gating control are shown in blue. (B) Median fluorescence intensity of T-BET on unstimulated CD4+ T cells from fetal intestinal lam. prop. (blue and red line; % T-BET+ of one donor in red included), infant intestinal lam. prop. (grey tinted line) and adult blood sample (black dotted line). (C)

- Gating controls of $CD127^{-}CD25^{+}$ $CD4^{+}$ Treg cells using fetal mesenteric lymph node (mes. LN) and infant PBMCs. (D) Gating controls of $FOXP3^{+}$ $CD4^{+}$ regulatory T cells from fetal mes. LN and infant PBMCs. (E) t-SNE plot of CD45RA and CD69 on $CD127^{-}CD25^{+}$ $CD4^{+}$ Treg cells from fetal and infant lam. prop. intestinal tissues.

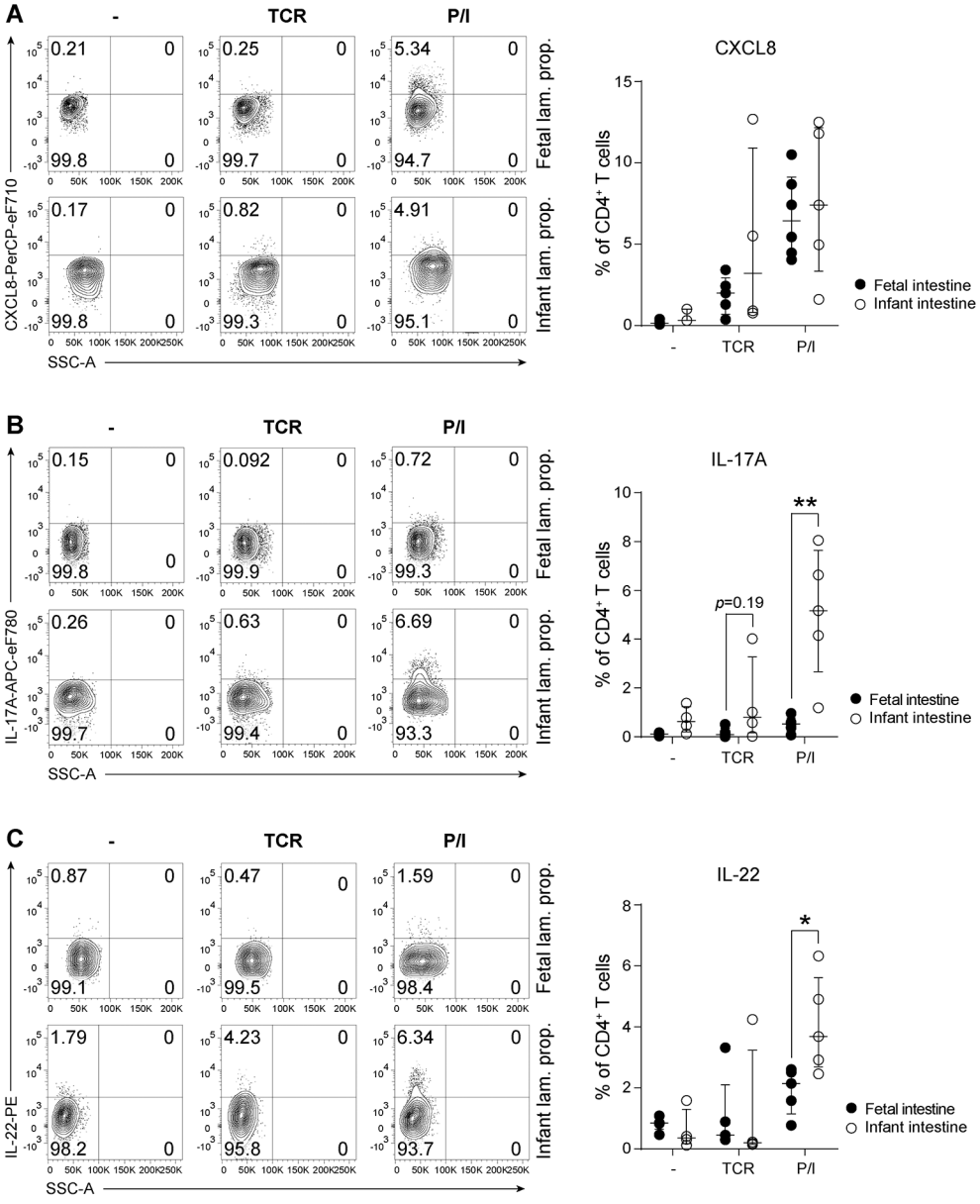

Figure S3. CXCL8, IL-17A, and IL-22 production is relativey low by fetal intestinal CD4+ T cells (see also Figure 3). (A) Representative flow cytometric plots and median percentage (± IQR) of lamina propria (lam. prop.)-derived CXCL8+CD4+ T cells unstimulated (-) or stimulated with anti-CD3 and anti-CD28 (TCR) or PMA-ionomycin (P/I) from fetal and infant intestines. (B) Representative flow cytometric plots and median percentage (± IQR) of lam. prop.-derived IL-17A+CD4+ T cells unstimulated or stimulated with TCR or P/I from fetal and infant intestines. (C) Representative flow cytometric plots and median percentage (± IQR) of lam. prop.-derived IL-22+CD4+ T cells unstimulated or stimulated with TCR or P/I from fetal and infant intestines. Mann-Whitney U comparisons. *p<0.05, **p<0.01. Fetal intestines (unstimulated and P/I n=6, TCR n=5), infant intestines (unstimulated and P/I n=5, TCR n=4).

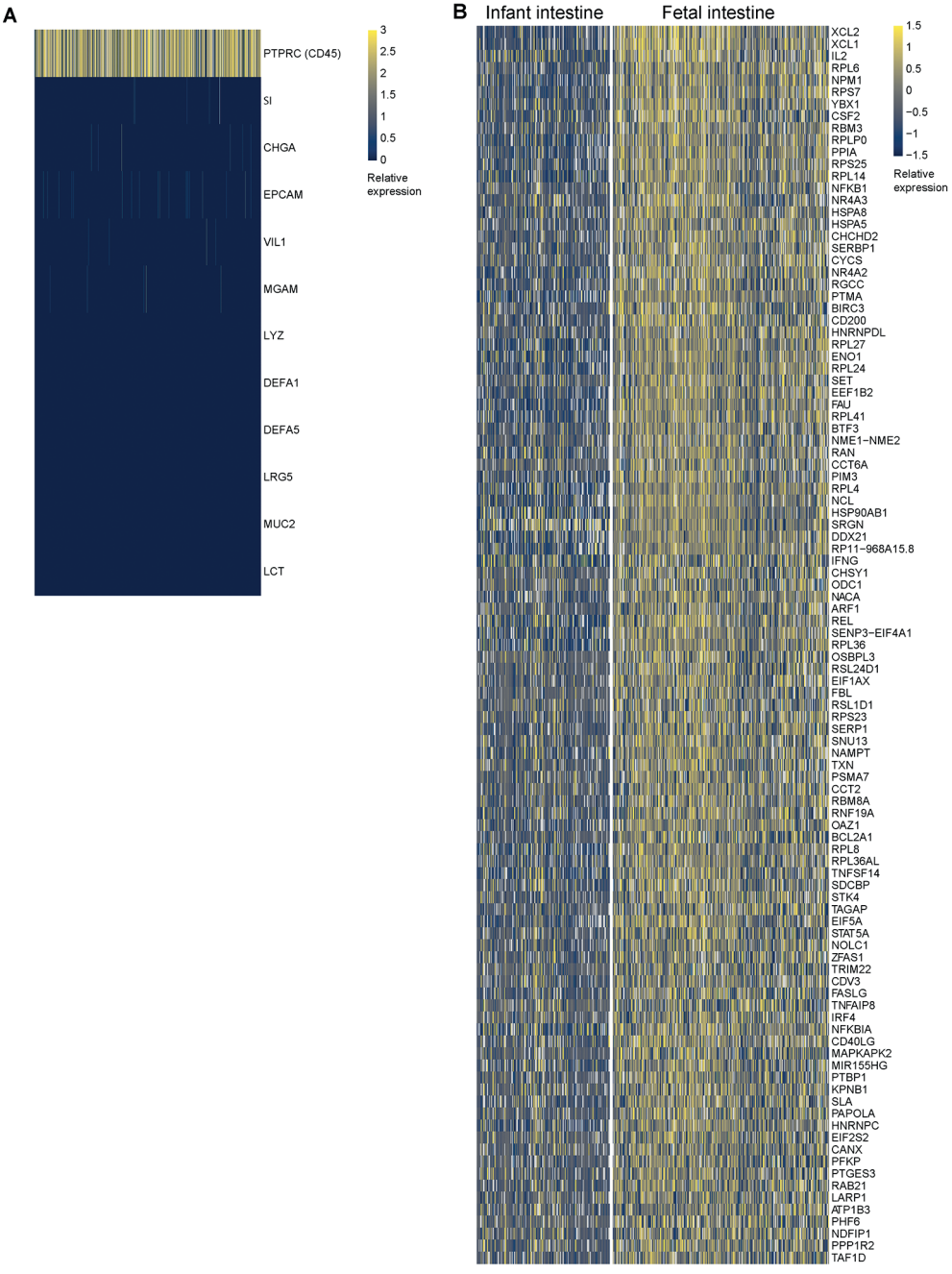

Figure S4. Single cell RNA-seq analysis of fetal intestinal CD4⁺ Tem cells indicates a Th1 phenotype (see also Figure 4). (A) Heatmap showing expression of hallmark genes of intestinal epithelial cells and immune cells (CD45) in sorted single fetal and infant cells assessed with scRNA-seq. (B) Heatmap showing 90 upregulated genes in PMA-ionomycin-stimulated fetal versus infant intestinal CD4⁺ effector memory (Tem) T cells. Fetal intestines (n=2), infant intestines (n=4).

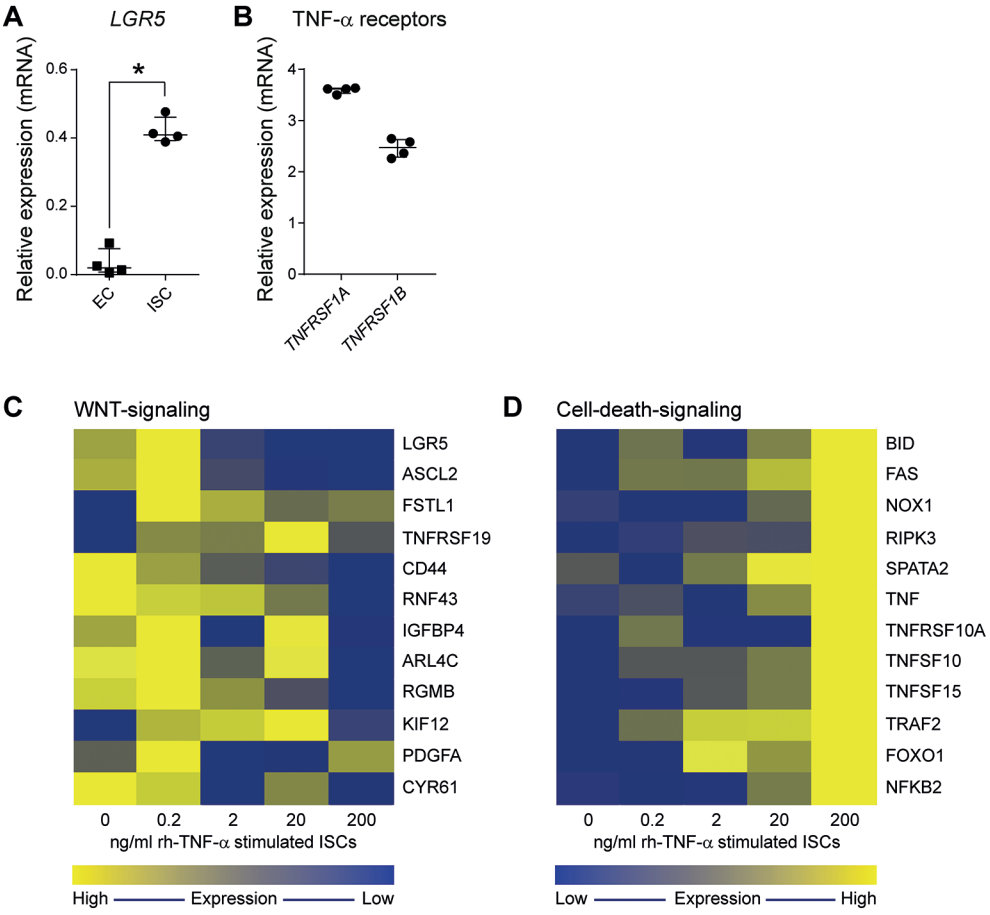

Figure S5. TNF-α mediates gene expression in fetal ISCs (see also Figure 5). (A) Relative expression of *LGR5* in fetal intestinal epithelial cells (EC) isolated from tissues compared to fetal intestinal stem cells (ISC) from organoid cultures of two donors assessed in duplicates. Median expression (± IQR) is shown. Mann-Whitney U comparison. (B) Relative expression of *TNFRSF1A* and *TNFRSF1B* in fetal ISCs from organoids at baseline of two donors assessed in duplicates. Median expression (± IQR) is shown. (C) Heatmap showing the median reads per kilobase per million (RPKM) of WNT target genes in ISC cultures stimulated with recombinant human (rh) TNF-α of two donors assessed in duplicates. (D) Heatmap showing median RPKM of cell-death-signaling genes in ISC cultures stimulated with rh-TNF-α of two donors assessed in duplicates.

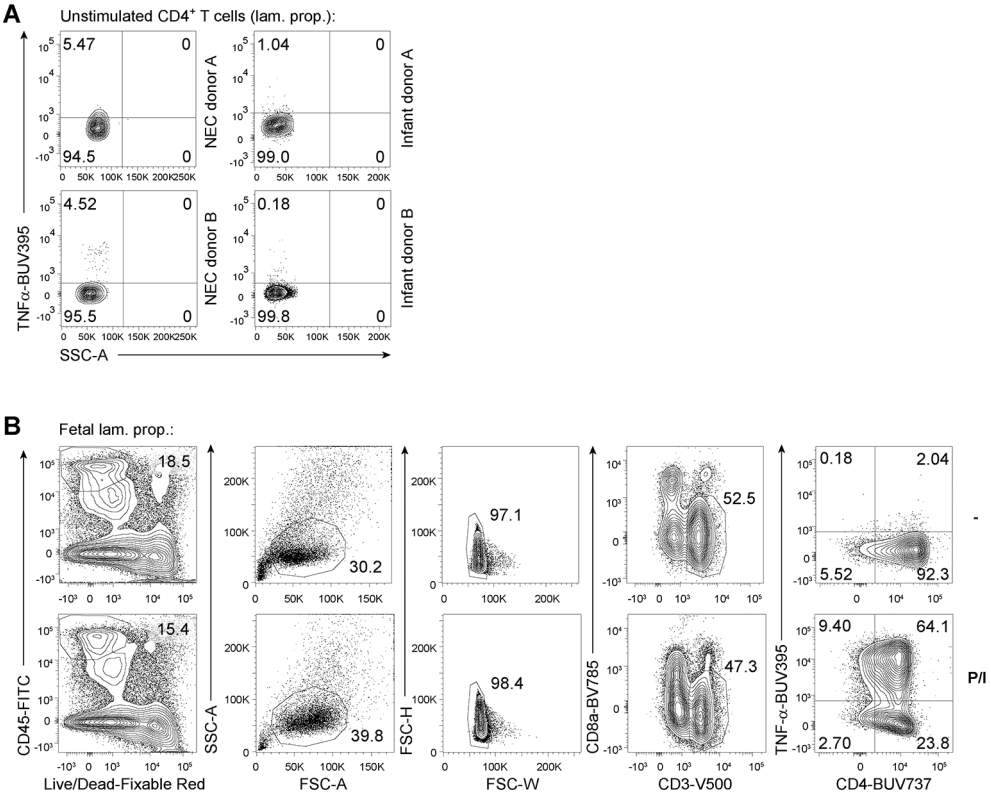

Figure S6. CD4⁺ T cells produce TNF-α at baseline in NEC intestinal tissues (see also Figure 6 and STAR Methods). (A) Flow cytometric plots of TNF-α-expression by unstimulated viable CD4⁺ T cells isolated from lamina propria (lam. prop.) intestinal tissues of two infants with NEC and two infants without NEC. (B) Gating strategy to determine CD4⁺ T cells upon PMA-ionomycine (P/I)-stimulation.

Table S1. Overview of all donors used in this study (see also STAR methods). Column 1: F=fetal tissues, I=infant tissues, P=premature infant tissues without NEC, N=Infant tissues with NEC=necrotising enterocolitis , A=adult blood. Columns 2 and 3: w=weeks, d=days, m=months, y=years. Column 4: U=unknown, M=male, F=female. Gender is unknown in the case of fetal tissue and blood donations.

Donor	Gestational age	Age at surgery	Gender
F1	16w	-	U
F2	17w	-	U
F3	18w	-	U
F4	16w	-	U
F5	17w	-	U
F6	18w	-	U
F7	15w	-	U
F8	19w	-	U
F9	20w	-	U
F10	18w	-	U
F11	14w	-	U
F12	20w	-	U
F13	15w	-	U
F14	16w	-	U
F15	17w	-	U
F16	17w	-	U
F17	16w	-	U
F18	18w	-	U
F19	20w	-	U
F20	14w	-	U
F21	18w	-	U
F22	20w	-	U
F23	19w	-	U
F24	18w	-	U
F25	17w	-	U
F26	16w	-	U
F27	13w	-	U
F28	20w	-	U
F29	20w	-	U
F30	17w	-	U
F31	18w	-	U
F32	18w	-	U
F33	16w	-	U
F34	19w	-	U
F35	16w	-	U
F36	17w	-	U
F37	16w	-	U
F38	20w	-	U
F39	17w	-	U
F40	16w	-	U
F41	17w	-	U

Table S1. (continued)

Donor	Gestational age	Age at surgery	Gender
F42	18w	-	U
F43	17w	-	U
F44	17w	-	U
F45	18w	-	U
F46	18w	-	U
F47	16w	-	U
F48	17w	-	U
F49	19w	-	U
F50	20w	-	U
I1	-	8m	M
I2	-	4m	F
I3	-	5m	F
I4	-	8m	F
I5	-	2m	M
I6	-	4m	F
I7	-	4m	F
I8	-	4m	M
I9	-	26m	M
I10	-	10m	M
I11	-	8m	M
I12	-	10m	F
I13	-	3d	F
I14	-	4m	F
I15	-	6m	M
I16	-	6m	F
I17	-	4m	M
I18	-	2m	M
I19	-	5m	F
I20	-	2d	M
I21	-	2m	M
I22	-	5m	M
I23	-	0d	U
I24	-	4m	M
I25	-	8m	M
I26	-	1m	M
I27	-	4m	F
P1	25w	5d	M
P2	26w	3d	F
P3	25w	12d	M
N1	24w	9w	M
N2	24w	11d	M
N3	33w	6d	M
N4	26w	5d	M
N5	24w	7w	M

Table S1. (continued)

Donor	Gestational age	Age at surgery	Gender
N6	26w	8d	F
N7	27w	7d	M
N8	24w	5w	M
N9	31w	2w	F
N10	28w	7w	M
N11	23w	8d	F
N12	23w	9w	M
N13	29w	7w	F
N14	25w	12w	F
A1	-	>18y	U